WELDING INSTITUTE OF CANADA
INSTITUT DE SOUDAGE DU CANADA

391 BURNHAMTHORPE ROAD EAST, OAKVILLE, ONTARIO L6J 6C9. Tel. (416) 845-9881

STUDY OF WELD CRACKING IN 2-1/4 Cr-1 Mo STEELS

RC93/4/84

Final Report

by

Welding Institute of Canada

This work was performed for the Physical Metallurgy Research Laboratories, CANMET, Energy Mines and Resources Canada under Supply and Services Canada Contract ISQ81-00078. The authors also acknowledge the guidance and valuable comments received from Dr. R. S. Chandel in the Scientific administration of the contract.

The views expressed in this report are those of the authors and do not necessarily reflect the views of CANMET.

DSS File Number:	17SQ.23440-1-9071
DSS Contract Serial Number:	ISQ81-00078
CANMET Project Number:	420502
CANMET Scientific Authority:	Dr. R. S. Chandel

March 1984

This report should be cited by Contract Report No: ISQ81-00078

DEC 19 1984

Crown copyright of this report is reserved.

MICROMEDIA

Approved by:

5/pp

Dr. Alan G. Glover
Director of Technology

STUDY OF WELD CRACKING IN 2-1/4 Cr - 1 Mo STEELS

by

Kam Shing Ko, Welding Institute of Canada

Robert B. Lazor, Welding Institute of Canada

EXECUTIVE SUMMARY

This project was undertaken to expand Canadian expertise in the fabrication of pressure vessels made from 2-1/4 Cr - 1 Mo steels. Weld cracking tests were conducted to ascertain the procedural variables and heat treatment conditions necessary to prevent transverse weld metal cracking. This report describes the results of Phase III of the work in which the G-BIG test was examined as to its usefulness as a "shop" test. Several joints were also welded using procedures recommended from the work and examined for cracking.

Cracking was encountered in the root pass of the G-BIG test and it was found that a preheat of 200°C was necessary to produce sound joints. However, since the G-BIG test tended only to give root cracking, it was not entirely satisfactory as a test which could be used to recommend procedures to avoid transverse weld metal cracking.

The joint simulation tests did not produce any cracking, even at very low preheat and interpass temperatures. This result was unexpected and prompted an evaluation of the consumables. It was found that the flux/wire combination used in this study gave very low levels of weld metal hydrogen and therefore cracking was not a problem.

The overall conclusion obtained in this study was that although intermediate heat treatments, post-weld heat treatments, and control of preheat and interpass temperatures are recommended, the conditions of the consumables are the most important parameter in preventing hydrogen-induced, transverse weld metal cracking.

TABLE OF CONTENTS

		Page
	Executive Summary	(ii)
	List of Tables	(iv)
	List of Illustrations	(v)
1.0	Introduction	1
2.0	Materials	2
3.0	Consumable Conditioning and Hydrogen Measurements	3
4.0	G-BIG Root Cracking Tests	4
	4.1 Instrumentation for G-BIG Tests	4
	4.2 G-BIG Test Procedures	5
	4.3 Effect of Fixturing Clamp	6
	4.4 Detection of Cracking	7
	4.5 Single Pass Welds	7
	4.6 Multipass Welds	9
	4.7 Summary of SMAW G-BIG Tests	13
	4.8 G-BIG Test With SAW	14
	4.9 Joint Simulation Tests	14
5.0	Discussion	15
	5.1 Gapped Bead-in-Groove Cracking Tests	15
	5.2 Joint Simulation Tests	18
6.0	Conclusions	19
7.0	Summary and Recommendations	20
8.0	References	22
	Appendix A LVDT versus time record for G-BIG tests	
	Appendix B Contraction results for multipass G-BIG test	
	Appendix C Welding Procedure Details	

LIST OF TABLES

		Page
1	Chemical Compositions of Materials	23
2	Hydrogen Measurements of Consumables	23
3	Summary of G-BIG Root Cracking Tests	24
4	Chemical Composition of OP41TT Submerged-Arc Flux	24

LIST OF ILLUSTRATIONS

		Page
Figure 1.	Details of test assembly and LVDT mounting for single pass, two pass and three pass welds	25
Figure 2.	Diagram of instrumentation for weld 7.	26
Figure 3.	LVDT output versus time for application and release of fixturing clamp	27
Figure 4.	Equivalent restraint model for G-BIG test.	27
Figure 5.	Effect of gauge length on contraction force.	28
Figure 6.	Contraction versus time for weld 2 as measured by LVDT 10. The arrow at E is representative of the expected behaviour when cracking occurs during the data acquisition period.	28
Figure 7.	Contraction behaviour of a single bead which did not crack within 800 s.	29
Figure 8.	Strain output from strain bridge 1 during deposition of the third layer of weld 7.	29
Figure 9.	Net strain versus time for weld 7, multilayer SMAW deposit, as recorded by strain bridge 1.	30
Figure 10.	Relationship between CaF_2 and $CaCO_3$ content in slag and diffusible hydrogen content in weld metal.	31

STUDY OF WELD CRACKING IN 2-1/4 Cr - 1 Mo STEELS

1.0 Introduction

In order to expand Canadian expertise in pressure vessel technology, a contract was obtained from CANMET/EMR to investigate the factors which affect cracking in 2-1/4 Cr - 1 Mo weld metals. The work plan submitted as CANMET /EMR Unsolicited Proposal UP-W-175 was expanded into three phases under a revised work statement which became the project guideline (CSN:ISQ81-00078).

During the project review of Phase I, it was agreed that the multiple pass G-BOP test would be useful to study transverse weld metal cracking, and Phase II was to proceed as outlined (1-4). The objective of Phase II was to establish crack/no crack conditions as a function of weld thickness, heat treatment, and hydrogen pick-up.

Since the tests involved welding in a machined groove with a gap between the two test pieces, the term G-BIG (gapped bead-in-groove) test was adopted. Three weld thicknesses of 13, 25 and 60 mm were examined. The 13 and 25 mm welds both exhibited similar transverse cracks which initiated at the gap between the two test blocks. Preheat temperatures of 160°C and 180°C were necessary to prevent transverse cracks for the 13 mm and 25 mm welds, respectively. The critical preheat temperature increased marginally when the weld metal hydrogen content was increased. The test assembly for the 60 mm welds consisted of four, instead of two blocks as with the other tests (5). This change was necessary because of difficulties which were encountered when trying to machine a deep notch. The cracks found in these latter welds were longitudinal cracks and no transverse cracks were observed. Nonetheless, this result was valuable in that it drew attention to the possibility of other forms of cracking. Since the objective was to establish crack/no crack conditions, this series of tests was continued and it was determined that a preheat of 200°C was necessary to prevent root cracking. Using lower preheat temperatures together with intermediate heat treatments was not effective as a means of preventing cracking because the cracks had already occurred before heat treatment.

A qualitative analysis of the results identified the problem of longitudinal root cracking to be the most critical when welding thick sections, and thus a preheat of 200°C appeared to be necessary. This preheat and interpass temperature would definitely prevent longitudinal cracks such as those observed in the G-BIG test.

The results obtained to date, combined with procedures outlined in the literature, were deemed sufficient to proceed with the representative welds in Phase III. The welding procedures were determined using the following philosophy:

1. Preheat to 200°C and maintain this interpass temperature to prevent root cracking.
2. Interrupt welding at selected times and conduct low-temperature (250°C - 300°C) intermediate heat treatments for hydrogen removal.
3. Complete welds and conduct low-temperature post-weld heat treatments. (LTPWHT)

At the request of the scientific authority, further G-BIG tests were conducted to determine whether this test method could be effectively used by fabricators as an inexpensive confirmation of welding procedures to preclude transverse cracking in 2-1/4 Cr-1 Mo weld metal.

This report describes the additional G-BIG tests and the weld procedure trials on representative full-thickness welds.

2.0 Materials

The 64 and 76 mm thick plates were supplied to ASME SA-387 Gr 22 Class 2 requirements, and delivered in the normalized (at 940°C) and tempered (675°C) condition. The reported chemical composition from the original mill test is listed in Table 1.

The reported chemical composition of the AWS E9018B3L shielded metal arc welding (SMAW) electrodes, 4 mm diameter, is also given in Table 1. The

electrode coating of the 9018B3L electrodes is a combination of $CaCO_3$, CaF_2, TiO_2, and SiO_2, with other compounds added in small amounts. The exact formulation is proprietary information but it is sufficient to know the major compounds in the coating. These electrodes were used for the root cracking examination for the G-BIG test, the multipass weld which was instrumented for strain and displacement, and for deposition of the root passes in the procedure tests. The root was welded with SMAW for the procedure welds to preclude the possibility of burn through or longitudinal weld centreline cracking which can occur in submerged arc welding of deep, narrow joints. The SMAW process was also chosen for the G-BIG tests because of the short weld length in the test piece.

Submerged arc welding of the simulated joints was conducted using 4 mm diameter OE-SD2 wire and OP41TT flux. The electrode composition and the subsequent weld metal chemistry are both listed in Table 1. Compared to the SMAW deposit, the SAW composition is slightly lower in carbon, manganese and silicon.

3.0 Consumable Conditioning and Hydrogen Measurements

Precautions were taken for handling and storage of the consumables to prevent contamination from atmospheric moisture. The hermetically sealed container of E9018B3L electrodes was stored after opening in an electrode oven at 125°C. The same temperature was used to condition the submerged arc flux for 16 hours immediately prior to welding.

The hydrogen contents of the weld metal deposits were measured using the method given by ISO3690, "Determination of hydrogen in deposited weld metal arising from the use of covered electrodes for welding mild and low alloy steels", which uses mercury as the eudiometric fluid. The results of the hydrogen measurements are given in Table 2. They confirm the low hydrogen designation for both of the consumables.

4.0 G-BIG Root Cracking Tests

The test procedure developed using G-BIG testing was found to be an effective means of examining root cracking in multipass welds (5). During these tests, it was determined that the time to cracking was an important variable. The onset of cracking was examined in this study for both single pass and multipass welds using instrumentation connected to the G-BIG blocks.

A total of seven G-BIG tests were conducted to determine the onset of cracking. The first three welds in the series were single pass deposits, the fourth and fifth tests were two pass deposits, the sixth weld was completed with three passes, and the final weld consisted of a total of twenty-eight passes. The preheat and interpass temperatures used in these tests ranged from 22°C to 100°C, as outlined in the following table:

Weld	Description	Preheat Temperature	Interpass Temperature
1	single pass	22°C	not applicable
2	single pass	50°C	not applicable
3	single pass	100°C	not applicable
4	two passes	50°C	50°C
5	two passes	50°C	50°C
6	three passes	50°C	50°C
7	28 passes	22°C	50°C

4.1 Instrumentation for G-BIG Tests

The instrumentation consisted of two LVDTs (linear variable displacement transducers) mounted on each side of the G-BIG test assembly as shown in Figure 1. Locknuts on the external threads of the LVDTs enabled the transducer to be mounted on a single U-shaped bracket on one of the 2-1/4 Cr-1 Mo blocks. The spring-loaded core bears on the surface of a projection on the other 2-1/4 Cr-1 Mo block. With this arrangement, the LVDTs are capable of measuring both expansion and contraction, and will be evident in the results. The LVDT excitation is provided by a 15 volt DC power supply.

Their output voltages are continuously monitored by a data acquisition system and recorded on magnetic cartridges. These signals are subsequently plotted as displacement versus time graphs using a sensitivity of 0.7874 volts/mm. The LVDT linearity is +/-0.15 percent of the full range of +/-12.7 mm. The LVDT excitation is such that a positive value represents contraction.

The axes of the LVDTs corresponded to the centreline of the root bead deposited in the groove. The LVDT channels were identified as outputs 10 and 11 for the data acquisition system. These numbers are utilized in the graphical outputs and in each case a sketch is provided to show the position of each LVDT in relation to the weld bead.

The final multipass weld to determine the onset of cracking in the G-BIG test was monitored using the LVDTs and four strain gauge half-bridges. The additional effort necessary to incorporate the strain gauges into the experiments was not warranted for the G-BIG tests with fewer passes. In those cases, sufficient information was obtained from the LVDT outputs. The overall assembly is shown in Figure 2. The half-bridge configuration provides self-temperature compensation and a bridge output of 1.3 times that available for a single gauge bridge. Compressive forces produced negative strain values and positive values of strain are due to expansion.

It is important to note that the LVDT and strain gauge outputs are opposite to one another as shown in the following table:

Instrumentation	Output Value	
	Contraction	Expansion
LVDT	positive	negative
strain gauge	negative	positive

This selection of positive and negative designation is consistent with the methods of data presentation in the literature.

4.2 G-BIG Test Procedures

The G-BIG consists of two blocks of the 2-1/4 Cr-1 Mo steel, one with a 0.85

mm recess machined on the face adjacent to the other block, which were clamped together before the test welds were made. The SMAW beads were deposited using 140 amperes, 21 volts, and a travel speed of 3 mm/s which gave a nominal heat input of 980 J/mm. The LVDT and strain gauge outputs were monitored for a total time of 800 s from the beginning of welding.

The 2-1/4 Cr-1 Mo steel blocks were preheated uniformly in an electrode oven prior to set-up in the fixturing device. The temperatures were monitored using chromel-alumel thermocouples placed in 25 mm deep holes adjacent to the groove in which the welds were deposited. After the blocks had cooled to room temperature, the clamp was released to observe whether or not the weld had cracked. If cracking had not occurred by this time, the clamp was reapplied and the weld was re-examined in 24 hours.

4.3 Effect of Fixturing Clamp

The purpose of the clamping the 2-1/4 Cr-1 Mo blocks together before the start of welding is to ensure a good contact between the adjoining surfaces and to prevent the blocks from rotating due to the shrinkage of the welds. It was recognized that there could be a possible influence of the clamping force on the resultant measurements and thus its effect was examined using LVDTs as in Figure 1. The two blocks were placed touching one another on the fixture base and the data sampling program was commenced to record the LVDT outputs for 800 s. The clamp was slowly applied to the blocks and released a total of three times, (Figure 3). In all cases it can be seen that the clamping force is constant because the contraction reaches a plateau of approximately 3.81 mm. This aspect is important since it demonstrates that the clamping force is uniformly applied for all of the tests. Another point worth mentioning is that the displacement returns to its original position after the clamp is released.

The exercise described above showed that the clamping fixture held the blocks as intended but did not address whether or not it affected the subsequent contraction. Prior to welding, the clamped blocks can be modelled as

in Figure 4(a). The clamping force, or preload P, maintains the blocks in contact. The surface contact on each side of the weld is equivalent to having the two 2-1/4 Cr-1 Mo steel blocks rigidly restrained with a 0.75 mm gap between them as in Figure 4(b).

If a weld were to be deposited in the bottom of the groove the weld would cause the blocks to move towards each other due to the shrinkage of the weld metal. A typical contraction curve would be given by the curve for ℓ = 1000 mm in Figure 5. If one assumes that an increase in clamping force would be equivalent to reducing the restraint length, then the results shown in Figure 5 for ℓ = 200 mm could be assumed. Since the contraction behaviour is identical and only varies in timing it can be concluded that a slight increase in clamping force would not affect the contraction results. Following along the same argument, it can also be stated that the clamping force would not affect the occurrence of cracking.

4.4 Detection of Cracking

Cracking due to hydrogen occurs by a series of discrete crack extensions and is commonly known to be a discontinuous mechanism. Crack advance occurs when local stress or hydrogen accumulations exceed a critical value. The toughness of the surrounding material is generally sufficient to arrest the crack and thus when considering the contraction or loading behaviour, a crack is detected whenever there is an abrupt drop in the contraction curve. This event should not be confused with the transformation expansion observed during cooling as at B in Figure 5, which is characterized by a more gradual drop in load. Therefore, any abrupt drops in the graphs of displacement versus time are considered to be representative of cracking events. An example of a weld bead cracking during the course of the data acquisition program is shown at arrow E in Figure 6.

4.5 Single Pass Welds

Three single pass welds were deposited using SMAW with preheat temperatures of 22, 50 and 100°C. The contraction versus time outputs

obtained for each weld for 800 s from the start of welding are shown in Appendix A. The visual examination of the welds after they had cooled to room temperature revealed that the two deposits welded at 22 and 50°C had cracked completely while the 100°C weld did not crack. Examination of this latter weld after 24 hours showed that it had cracked sometime after it had cooled to room temperature.

It is commonly accepted that hydrogen cracking is influenced by preheat and this is measured by the time to cool to 100°C, t_{100}. The times obtained for t_{100} were 29, 454, and 1676 s for preheats of 22, 50 and 100°C, respectively. Therefore, considering the 800 s recording time, it was expected that examination of the LVDT outputs should indicate any initiation of cracking.

The contraction curve of weld 3 shown in Figure 7 is representative of a weld which did not visibly crack within 800 s. The events at points A, B, C and D can be described with reference to the weld deposition and resultant shrinkage. The abrupt expansion at point A signals the time at which the weld moves from one block to the other. The heat of welding causes the baseplates to heat up and expand during welding. As soon as the weld has been completed, point B, the G-BIG assembly now begins to cool from some peak temperature and the LVDTs register this contraction. The transformation expansion of the weld metal produces a drop in the contraction-time curve at point C. The subsequent contraction continues to point D. Comparing the outputs on either side of the 2-1/4 Cr-1 Mo blocks, there is a difference between LVDT 11 and 10 during the deposition of the weld but both LVDTs register a final contraction of 0.0762 mm. The discrepancy during welding could be due to the arc energy being more concentrated on the LVDT 10 side of the groove or the two sides may not have been subjected to the same preload. Past experience with contraction measurements suggests that the arc energy effects are the most probable cause, but this difference was also considered to possibly indicate a cracking event. Therefore, the two criteria of an abrupt load drop and difference in LVDT behaviour was used to judge whether or not cracking could be predicted from these graphs while visual examination was used for confirmation. It is likely that weld 3 cracked within the 800 s period, but this was not confirmed visually.

Looking now at the results for welds 1 and 2, (see Appendix A) and knowing that they cracked within 800 s, the outputs were examined to ascertain whether or not the LVDTs could detect crack initiation. The weld 2 results indicate that welding started at 21 s, contraction of the LVDTs began about 34 s, at 37 s there was an abrupt change in contraction (point E), after which the contraction progressed as expected. The final value of LVDT 10 was 0.127 mm while LVDT 11 was actually a negative value of -0.0625 mm. Therefore, both the loading drop at E and the difference in the final LVDT readings were thought to be indications of crack occurrence in the G-BIG test.

The curves for weld 1, which was know to have cracked within 800 s, did not exhibit a load drop as at E for weld 2 but the final values of displacement, 0.046 mm for LVDT 10 and 0.0102 mm for LVDT 11, were considered to have been different because of the cracking. The small indication at F for LVDT 10 (Weld 1) could have been the point of crack initiation, even though it was not as obvious as point E for weld 2. The cracking could have been recorded only by LVDT 11 for weld 1, as possibly shown for the non-uniform loading after the transformation expansion (between G and H). This behaviour was the only obvious anomoly in the contraction curves which could have registered the cracking which was known to have been 100%.

After this initial examination for the single pass weld, two and three pass welds were deposited in the G-BIG grooves and their contraction behaviour was examined.

4.6 Multipass Welds

The next series of tests involved three welds deposited using SMAW and 50°C preheat. One of the aims was to determine the effects of bead placement on the contraction versus time plots obtained using the LVDTs. More importantly, however, these tests were to examine the effects of subsequent weld passes on the occurrence of cracking in the G-BIG test.

The bead deposition sequence and contraction curves are shown in Appendix A for each weld. In all cases, the first pass was deposited in the centre of the groove. For weld 4 the second pass was deposited on the LVDT 10

groove side, while for weld 5 the second pass was laid on the LVDT 11 side of the groove. For weld 6, the second pass was on the LVDT 10 side and the third pass was on the side of LVDT 11. The following section will discuss and compare each of these tests.

The start and end of each of the passes is shown on the graphs in Appendix A for welds 4, 5 and 6. An obvious difference between these results is the apparently lower sensitivity of the LVDTs in monitoring the contraction of the first pass in the multipass welds compared to the single pass deposits. However, since only the qualitative behaviour of the joint was being investigated, it was not examined further.

In welds 4 and 5, the positioning of the second weld bead is seen to affect the LVDT outputs. For weld 4, in which the second bead was deposited on LVDT 10 side, the greatest expansion during welding is recorded for the opposite side, LVDT 11. Similarly, for weld 5 where the second bead is laid on the LVDT 11 side, the opposite side, LVDT 10, experiences the greatest expansion during welding. From these observations, it was seen that the side on which the weld was made acted as a hinge point and the effects of expansion were amplified for the other LVDT. The same trend was observed for weld 6 which was completed in three passes in that the largest variations were observed for the transducers on the side opposite to welding.

As previously mentioned, these tests were to be examined for the influence of subsequent deposits on weld metal cracking. This was done by studying the curves in Appendix A. For welds 4 and 5, the curves did not clearly indicate any changes in the contraction records which would be indicative of cracking. The only possible cracking event observed on the curves for the multipass welds was at the 50 and 60 s points at J and K for weld 6. The remaining portions of the curves did not indicate further cracking. Visual inspection once the weld had cooled to room temperature did not reveal extensive cracking, but examination after 24 hours resulted in an observation of 90% cracking.

The results of welds 4, 5 and 6 showed that deposition of subsequent welds immediately after completion of the root bead was effective in delaying weld metal cracking for a short time, but complete cracking was observed within 24 hours.

A subsequent extension of this multipass weld study was to determine whether cracking would still occur for a typical multilayer weld. It was possible that the heating effects of the subsequent deposits would assist in the removal of hydrogen from the root beads and prevent cracking. This multilayer G-BIG test (weld 7) used the LVDT and strain gauge instrumentation shown in Figure 2. Welding was commenced with the 2-1/4 Cr- 1 Mo baseplates at room temperature, while a minimum 50°C interpass temperature was maintained. Strictly speaking though, the interpass temperature was actually an interlayer temperature. In order to record data on magnetic tape without having to modify the program for each pass, it was advantageous to deposit a complete layer for each reloading of the data acquisition program. Thus, when the 2-1/4 Cr - 1 Mo blocks cooled to 50°C another weld layer was deposited with the actual interpass temperature slightly increasing with each pass, up to a maximum of 90°C. The subsequent layer would be commenced when this temperature became 50°C through natural cooling. The results of this final G-BIG test welded with SMAW electrodes was recorded in a total of six storage files, as shown in the table below:

Summary of Storage Files for Weld 7

File Name	Weld Layer	Passes
7A	1, 2	1, 2, 3, 4
7B	3	5, 6, 7
7C	4	8, 9, 10, 11
7D	5	12, 13, 14, 15,16
7E	6	17,18,19,20,21,22
7F	7	23,24,25,26,27,28

The graphs of the transducer and strain gauge bridge outputs are given in Appendix B. The start of welding of each pass is marked by a circled number. The numbering of each output graph is identified by the file name

and the channel identification. For example, 7A4 identifies strain gauge bridge 4 for weld layers 1 and 2, while 7D10 identifies LVDT 10 for the fifth layer. The relative positions of the strain bridges and LVDTs are shown in Figure 2.

A typical strain output for the welding of a layer (file 7C) is shown in Figure 8 for strain bridge 1. The behaviour of bridge 3, which was directly across from bridge 1, was identical to that shown in Figure 8 except that its magnitude was smaller. With reference to Figure 8, it was possible to describe the effects of welding on the resultant measurements. Soon after welding commenced, the temperature rise in the 2-1/4 Cr-1 Mo blocks caused them to expand, which in turn removed some of the preload on the strain gauge bridges. This heating expansion was registered as a positive strain increment. As the heat dissipated away from the weld, the effect was reversed. Contraction of the bead during cooling resulted in the strain values becoming negative. With each subsequent pass there was a corresponding positive and negative strain fluctuation. At the completion of this layer, the cooling of the G-BIG blocks resulted in a net contraction, or a 'net strain' which was negative. In some instances the net strain was positive for a layer but the final strains for each bridge were all negative, or indicating contraction.

In all of the strain gauge output graphs, there was no evidence of abrupt load drops which would have indicated the occurrence of cracking. The LVDT outputs of these welds did not indicate cracking either.

The 'net strain' values for weld 7 are listed in Appendix B and shown in Figure 9. Although the residual stresses increased with each additional layer, the 'net strain' increment was diminished owing to the increase in net section area.

Weld 7 was subsequently sectioned both longitudinally and transversely in the vicinity of the notch between the G-BIG blocks. Subsequent examination at up to 500 X magnification did not reveal any cracks. This result using only a 22°C preheat and 50°C interpass temperature was unexpected in comparison to the G-BIG tests in Phase II of this project (5). The main difference be-

tween these tests were the procedures used for the first couple of welds deposited in the root. In the previous tests (5), the interpass temperature was observed between each weld while for weld 7 the first four beads were completed before the root was allowed to cool. The rapid succession of beads for weld 7 was thought to have been sufficient to prevent cracking by maintaining the temperature above 100°C long enough for cracking to have been prevented. The slower cooling cycle allows hydrogen to diffuse away from the susceptible regions which, in this case, are at the root notch. With a lower resultant hydrogen content, the susceptibility is reduced and cracking is thus prevented.

The improved crack resistance of weld 7 agrees with the results of the G-BIG tests described in the previous sections (Table 3). The root cracking observed with the single pass welds with preheats up to 50°C was delayed if a second bead was deposited immediately after the root bead. Reducing the preheat to 22°C and depositing a total of three beads essentially prevented cracks from developing within 24 hours. This multipass deposit (weld 7) can be seen as an extension of this series and demonstrates the importance of weld sequence and temperature build-up in preventing hydrogen-induced cracking which could initiate from notches in the root region of multipass welds.

4.7 Summary of SMAW G-BIG Tests

In this report, and the previous study (5), root cracks were observed both parallel and transverse to the welding direction, depending on the type of notch. The cracks were prevented in multipass deposits if subsequent welds were deposited before cracking had initiated in the root region. This procedure allowed welds to be deposited even with the 2-1/4 Cr - 1 Mo blocks at room temperature at the start of welding. However, if a minimum interpass temperature was observed and the time between deposition of successive beads was increased, then it was found that a minimum 200°C preheat and interpass temperature was necessary to prevent longitudinal root cracking. A preheat of 160°C was sufficient to prevent transverse root cracking in multipass deposits.

4.8 G-BIG Test With SAW

A G-BIG test was conducted using a 4 mm diameter OE-SD2 wire and OP41TT flux, submerged arc welding consumables. The primary reason for this test was to compare one-sided SAW to SMAW procedures. The G-BIG test assembly with a 75 mm weld thickness was used for this test, weld 8. The root pass was deposited using a nominal heat input of 2.16 kJ/mm with a preheat temperature of 150°C. All subsequent passes (2 to 48) were deposited with an interpass temperature of 200°C and a heat input of 2.40 kJ/mm. The weld was sectioned and examined 24 hours after it had been completed. A longitudinal root crack approximately 2 mm deep was found along most of the length of the weld. This result confirmed the previous G-BIG test conclusions in that a preheat temperature of 175°C was insufficient to prevent longitudinal root cracking. The SAW deposit therefore gave similar crack susceptibilities as the SMAW deposits.

The longitudinal cracking observed in both the SAW and SMAW procedures drew attention to the importance of a sound root bead with good penetration. The longitudinal seam with incomplete root penetration is susceptible to root cracking and should be avoided. Therefore, in the subsequent joint simulation welds, a SMAW root bead was deposited to ensure adequate root penetration. A preheat of 200°C was employed to prevent cracking. Because of differences in the compositions of the SMAW and SAW deposits, the SMAW root beads were removed by back gouging before the second side was welded.

4.9 Joint Simulation Tests

In order to evaluate the results of the G-BIG tests, typical joints were prepared and welded based on their results. The welds were made on 100 mm thick plates using the procedures listed in Appendix C. Welds 9 and 10 were double bevel joints which were not restrained while weld 11 was a single bevel joint which was restrained from rotation using strongbacks. The use of the strongbacks prevented the SMAW root from being back-gouged.

The completed weld beads were cooled in still air and left to cool 24 hours before examination. Microscopic examination of transverse and longitudinal sections confirmed that the recommended welding procedures prevented hydrogen cracking.

5.0 Discussion

The emphasis in this final phase of the project was to investigate the G-BIG test in terms of its usefulness as a shop floor test in terms of its ability to confirm welding procedures to avoid transverse weld metal cracking for welds of representative thicknesses. The discussion will also address the approach necessary to prevent this particular problem in welded construction.

5.1 Gapped Bead-in-Groove Cracking Tests

One of the most frequent concerns during welding is the assurance that an approved welding procedure will preclude possible problems such as cracking. A common experience during fabrication is the apparently greater susceptibility of some joint types or heats of steel to cracking, either in the weld metal or the heat-affected zone. Over the years, fabricators have been able to successfully prevent many problems by implementing small, inexpensive tests into material specifications and/or quality control procedures. Some of these proven methods include Tekken tests, controlled thermal severity (CTS) tests, cruciform tests, and gapped bead-on-plate (G-BOP) tests. A common element throughout the myriad of test methods available is that they primarily are concerned with the problems of hydrogen-induced embrittlement.

In any hydrogen cracking test the principal variables are hydrogen content, stress, and preheat. The procedures followed in a given test remain constant with one variable, usually preheat, varied at any one time. Depending on the complexity of the procedure and the interpretation of the results, one can combine these values with past experience for a good indication of recommended welding parameters. From a fabricator's viewpoint, an optimum test would be one that did not require extensive metallography or ancillary equipment. The G-BOP test is a prime example of this point since good reproduc-

ibility at reasonable cost is achieved (2). The gapped bead-in-groove (G-BIG) test showed promise (3) as a comparable multipass test method and as such, it was further studied in this project. The following discussion describes the rationale and reports on results of examining the factors involved in the G-BIG test.

Initial trials (4) to study multipass transverse weld metal cracking gave positive indications that the G-BIG test was a valid method for investigating hydrogen-induced transverse cracking in 2-1/4 Cr-1 Mo steel welds. This conclusion was drawn since cracking was shown to be controlled by preheat which acts to reduce the hydrogen content of the weldment and the stress, to some extent.

The report (5) on phase II of this project used the G-BIG test to establish crack/no crack conditions in the weld metal as a function of weld thickness, hydrogen content, and studied the effectiveness of low temperature, post-weld heat treatments. The two smaller welds, 13 and 25 mm deep, gave good crack indications transverse to the welding direction with initiation occurring at the gap between the two blocks. The preheat temperatures to prevent transverse cracks increased with greater weld thicknesses (higher stress) and with greater initial hydrogen contents. The configuration used for the 60 mm welds employed four, instead of two, blocks and this resulted in the formation of longitudinal cracks. Although not anticipated, this result drew attention to the commonly encountered problem of root cracking when welding thick sections. A preheat temperature of 200°C was found to be necessary to prevent these cracks. Lower preheat temperatures and intermediate heat treatments were ineffective because the LTPWHTs were not commenced soon enough after welding to prevent root crack initiation. Based on these observations, welding procedures were recommended using high initial preheat temperatures with lower interpass temperatures once a sound root region was ensured. Overall, the susceptibility of 2-1/4 Cr - 1 Mo steels was shown to be a function of hydrogen content and preheat temperature.

At the end of Phase II, the direction of the project turned to a detailed investigation of the G-BIG test itself. Instrumentation techniques with

strain-gauged blocks and displacement transducers were used to study the mechanics of the testing method, and this led to some interesting results.

It was not determined whether or not the LVDTs employed in the instrumented G-BIG tests were sensitive enough to detect crack initiation in all cases. It has been shown that cracking sometimes started soon after welding finished and some initiation events were detected by the LVDTs even before the weld cooled to room temperature. In these cases cracking was noted within 30 s of completion of the weld. The single pass welds at preheats of 22°C and 50°C cracked immediately and completely. At 100°C preheat, the weld cracked 100% after 24 hours. Visual inspection immediately after welding did not reveal any cracking but crack initiation was assumed from the LVDT records. At the higher preheat, although cracking was delayed, it was not prevented, indicating that a preheat greater than 100°C is required.

The tests with two passes and three passes were conducted at 50°C. The equivalent single pass welds made using this preheat exhibited 100% cracking almost immediately after welding while the multipass welds cracked 100% somewhat later but still within 24 hours. This indicates that the subsequent passes had delayed the cracking in the root pass. It was also seen that most crack initiation took place within 30 s after welding. If cracking does not occur in the interval between the root pass and the subsequent pass the likelihood of cracking is reduced if the weld is completed without delay. The subsequent passes act to temper the weld which relaxes the stress, produces less susceptible microstructures, and allows more time for hydrogen to diffuse away from the weld. In view of this, a tandem arc welding process may be beneficial since the trailing arc can be set up following the leading arc, well within 30 s and deposit a tempering bead before cracking initiates. The main purpose, however, of this trailing arc would be to remove the hydrogen from the weld area and reduce the possibility of hydrogen-induced cracking, provided that a critical hydrogen concentration is not exceeded. The tempering effect is obvious in the multipass welds and was indicated by the instrumented G-BIG test, weld 7. Each time a pass is deposited, the strain imposed across the joint would rise to a certain value and would fall when the next pass was started. Thus as long as there is more than one pass in a joint there are tempering beads available. However, not all of the imposed restraint could be released as the number of passes increased, especially in the last passes on the final layers where the restraint forces are

the highest. Therefore, some sort of stress relieving must be applied to relax the restraint imposed on the last few layers.

In summary, the use of the G-BIG test did prove to be useful for obtaining general guidelines for prevention of hydrogen-induced cracking but root cracking was identified as possibly being a more important problem. It should also be pointed out that the nature of the cracking typified in the G-BIG test was markedly different than that normally associated with transverse weld metal cracking (6).

5.2 Joint Simulation Tests

The welding procedure recommendations outlined in the phase II report (5) were applied to representative full thickness welds. As previously mentioned in section 2.2.3, none of the welds exhibited transverse cracking, even those with lowest preheat and interpass temperatures. At first it was considered that the unrestrained joint did not impose sufficient stress along the weld for cracking to occur. This was examined by making a restrained weld using low preheat, weld 11. Since this did not produce any cracking it was obvious that some other factor was necessary to explain the results. With preheat and stress having already been considered, this meant that the diffusible hydrogen content of the flux/wire combination was the only variable remaining.

The diffusible hydrogen contents measured for the conditioned flux are 10.51 ml/100 g deposited metal, or 2.20 ml/100 g of fused metal. The values are equivalent to 7.62 ml/100 g deposited metal, or 1.22 ml/100 g fused metal measured under glycerin. These results show that the flux/wire combination produces a resultant hydrogen level which is within the low hydrogen designation, <10 ml/100 g deposited metal when measured under glycerin. The OP41TT flux contains a high quantity of CaF_2 and $CaCO_3$ (see Table 4). These two compounds readily generate gases whose subsequent decomposition lower the partial pressure of hydrogen in the arc cavity (7). The reduction in weld metal diffusible hydrogen with increases in CaF_2 and $CaCO_3$ has been

reported (7) as shown in Figure 10. Additions of CaF_2 or $CaCO_3$ up to 15% are effective in reducing the hydrogen content by one-third.

The hydrogen of the fused part of the weld is the important value when considering hydrogen cracking. In multipass welds, the maximum hydrogen content is obtained just below the last weld to be deposited. This value saturates after about five beads to the hydrogen content of the fused metal of a single bead. For the conditioned OP41TT flux used in the present study, the maximum hydrogen content below the final bead would be 1.22 ml/100 g of weld metal (glycerine). In a study which measured diffusible hydrogen distributions through the thickness of completed welds (8), it was found that transverse cracks could be prevented if the peak hydrogen contents could be reduced below 3.3 ml/100 g (in glycerine) through the use of post-weld heat treatments. Therefore, with the low hydrogen contents of the baked OP41TT, and the use of moderate preheat and interpass temperatures, low hydrogen conditions were maintained during the joint simulation welds and hydrogen-induced cracking was prevented.

The results of this phase of the study have shown that weld metal cracking in 2-1/4 Cr-1 Mo steels can be prevented through the use of low preheat and interpass temperatures in conjunction with good welding practices and consumables with very low hydrogen contents. Yet in actual practice, one should still be cautious since hydrogen contents vary and there are frequently highly-stressed locations in fabricated components. These locations would likely cause cracking at the same preheat as welds located in lower stress regions. This is indicated by weld 8, where preheat and interpass temperatures were as high as 200°C and yet there still was cracking near the vicinity of the root. Moreover, the cooling rates expected in large fabricated components are much higher than laboratory test pieces and the restraint conditions also differ. In addition, welding procedures are not always followed exactly in actual practice due to labour and environmental factors. Therefore, the preheat temperature obtained from Phase II, although somewhat conservative should be followed in practice to prevent cracking.

6.0 Conclusions

1. The LVDTs provided a method to detect crack initiation in the G-BIG test which was impossible by visual inspection. The interpretation of the cracking event, however, was not exact due to coexisting weld mechanics effects.

2. The restraint imposed across a weld joint increased with the increase in the number of passes. The increment per layer gradually decreased as the number of weld layers increased.
3. Every hot pass in a multipass weld had a stress-relieving effect on the previous pass and had a tendency to stop or delay cracking.
4. A tandem arc process may be beneficial for stopping crack initiation.
5. A crack-free weld can be obtained at lower preheat and interpass temperatures with the employment of a flux containing high percentages of CaF_2 and $CaCO_3$.

7.0 Summary and Recommendations

This report by itself addresses the third and final phase of a study which has examined the factors which affect transverse weld metal cracking in 2-1/4 Cr-1Mo steels. The first phase report summarizes the literature on hydrogen-induced, weld metal cracking, describes the results of single pass weld metal cracking tests, and shows the validity of the G-BIG test to examine cracking in multipass welds. Phase II was involved with establishing crack/no crack conditions as a function of weld thickness, heat treatment, and hydrogen pick-up. In Phase III, the effectiveness of low temperature post weld heat treatments was to be examined as a means to prevent transverse weld metal cracking on representative full thickness welds (100 mm).

The results of Phase I showed the dependence of weld metal cracking on hydrogen effects and discussed how the welding procedures influence the crack susceptibility.

In the second phase, the results showed that longitudinal root cracking could possibly control the overall joint integrity. Preheat temperatures of 200°C were required to prevent these cracks, and no transverse weld metal cracks were observed. It was found that the high preheat temperature was necessary to prevent root cracking, and was to be used in the representative welded joints.

The welds in Phase III were made with a sound root and welded with submerged arc consumables using various thermal treatments. Even with very low preheat and interpass temperatures, transverse weld metal cracking was not observed. This result was attributed to the exceptionally low hydrogen content of the particular consumables. From phase III, weld metal cracking did not present itself as a problem in 2-1/4 Cr-1Mo steels. However, past experience, as described in Phase I, has attached paramount importance to transverse weld metal cracking. Therefore, the present results indicate that careful control of welding procedures and maintaining extra low hydrogen conditions are effective means to produce sound weldments. This has been emphasized in the final phase report.

Overall, this study has identified the nature of the problem, tests have been conducted to quantify the effect, and the importance of low hdrogen consumables has been established. In light of the evidence presented, the problem of hydrogen-induced cracking during fabrication using 2-1/4 Cr-1Mo steel can be prevented, but obviously is a major problem for many fabricators. This situation is compounded further by the fact that defects, when found, are very often repaired without determining their cause. At this point, it may be instructive to perhaps review, in light of these and previous (4, 5) results, the overall incidence and location of cracks in 2-1/4 Cr-1Mo weld metals. Without the information which would accrue from such an exercise, it would be impossible to provide a definitive approach to welding of 2-1/4 Cr-1Mo steels and ensure that hydrogen cracking would not be a problem.

8.0 References

1. K. Satoh and S. Matsui, "Reaction Stress and Weld Cracking Under Hindered Contraction", IIW Doc IX-574-68.

2. R. B. Lazor, "Study of Weld Cracking in High Strength, Low Alloy Steels", Welding Institute of Canada Report RC13/80, CANMET Project Number 8-9073.

3. B. A. Graville, private communication.

4. R. B. Lazor, "Weld Cracking in 2 1/4 Cr - 1 Mo Steel, Phase 1", Welding Institute of Canada Report RC93, CANMET Project Number 420502.

5. R. B. Lazor, "Weld Cracking in 2 1/4 Cr - 1 Mo Steels, Phase 2", Welding Institute of Canada Report RC93/2/83, CANMET Report Number ISQ81-00078.

6. E. Takahishi and K. Iwai, "Prevention of the Transverse Cracks in Heavy Sction Butt Weldments of 2 1/4 Cr - 1 Mo Steel Through Low-Temperature, Post-Weld Heat Treatment (Report 1)", Trans. of Japan Welding Society, Vol 10 (1), April 1979, p 46.

7. Y. Ito, M. Nakanishi, N. Katsumoto, and H. Tsumura, "New Submerged Arc Welding Technique for 2 1/4 Cr-1 Mo Thick Plates", IIW Doc. IX-1193-81.

8. E. Takahashi, K. Iwai, and T. Horitsuji, "Prevention of the Transverse Cracks in Heavy Section Butt Weldments Through Low Temperature Postweld Heat Treatment (Report 4)", Trans. of Japan Welding Society, Vol II (2), October 1980, p 13.

9. R. B. Lazor, "Collaborative Study on Hydrogen", Welding Institute of Canada Report RC25/2/79, November 1979.

TABLE 1

CHEMICAL COMPOSITION OF MATERIALS

Sample	Chemical Composition, wt.%						
	C	Mn	Si	S	P	Cr	Mo
Plate	0.11	0.43	0.27	0.015	0.014	2.29	0.91
OE-SD2 electrode	0.12	0.55	0.17	0.012	0.011	2.10	0.900
Weld Metal	0.065	0.38	0.10	0.006	0.010	2.06	0.88
E9018-B3 electrode	0.04	0.80	0.35			2.20	1.05
Weld Metal	0.08	0.60	0.30			2.1	0.98

TABLE 2

HYDROGEN MEASUREMENTS OF CONSUMABLES

Electrode	Condition	Hydrogen Content, ml/100g	
		Deposited Metal	Fused Metal
E9018B3L	as received	2.42	1.31
0E-SD2/OP41TT	as received	15.89	3.41
0E-SD2/OP41TT	stored at 125°C for 16 h	10.51	2.20

TABLE 3

SUMMARY OF G-BIG ROOT CRACKING TESTS

Weld	Preheat Temperature °C	Interpass Temperature	Number of Passes	Results		
				t_{100}	t_{50}	
1	22	-	1	29	80	cracked 100% at 30s
2	50	-	1	454	2743	" 100% at 15s
3	100	-	1	1676	6948	" 100% within 24 h
4	50	50	2	454	2743	" 100% within 24 h
5	50	50	2	454	2743	" 100% within 24 h
6	50	50	3	454	2743	" 90% within 24 h
7	22	50	28	29	80	" 5% within 24 h

TABLE 4

CHEMICAL COMPOSITION OF OP41TT SUBMERGED-ARC FLUX (7)

BI = 3.1					
SiO_2	CaO + MgO	Al_2O_3	MnO	CaF_2	TiO_2
13	35	15	0.2	30	0.5

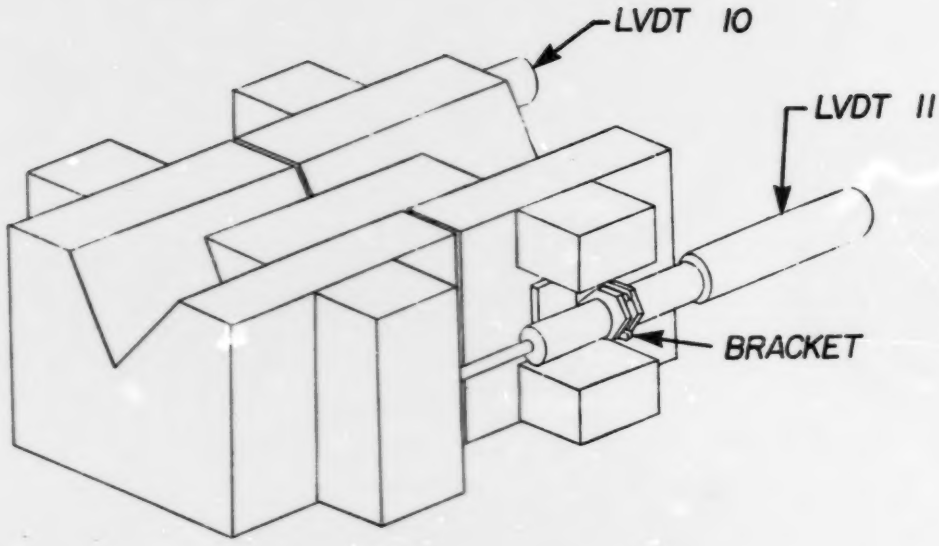

Figure 1. Details of test assembly and LVDT mounting for single pass, two pass, and three pass welds.

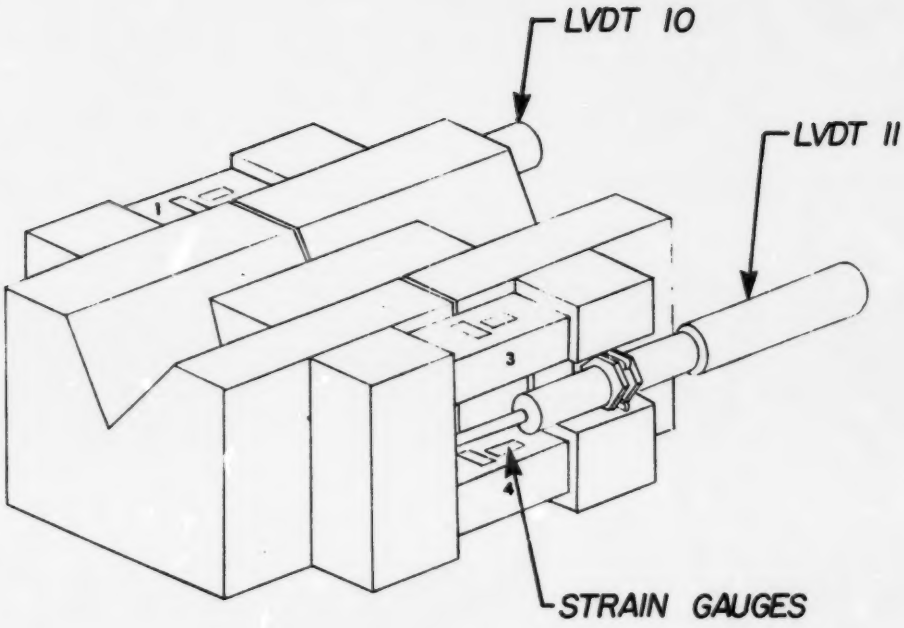

Figure 2. Diagram of instrumentation for weld 7.

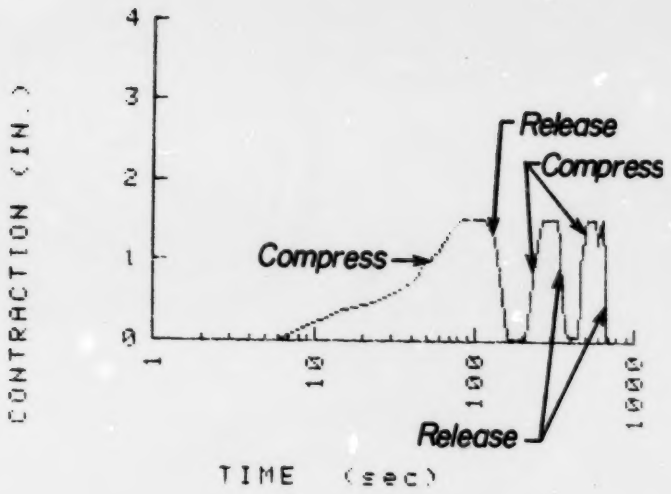

Figure 3. LVDT output versus time for application and release of fixturing clamp.

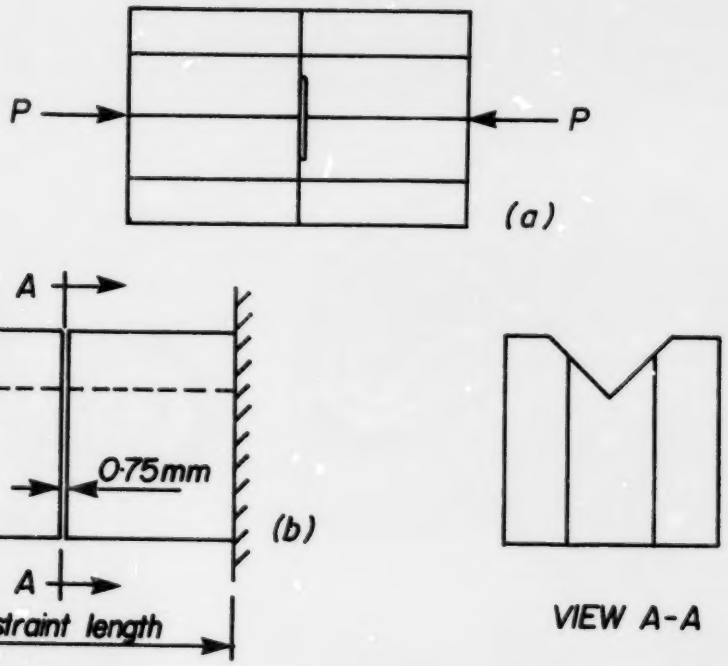

Figure 4. Equivalent restraint model for G-BIG test.

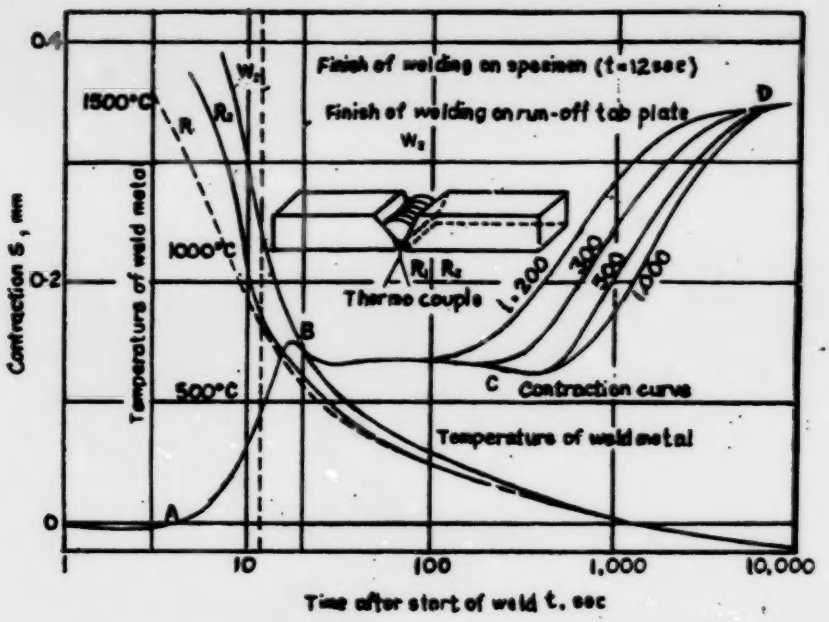

Figure 5. Effect of gauge length on contraction force (1).

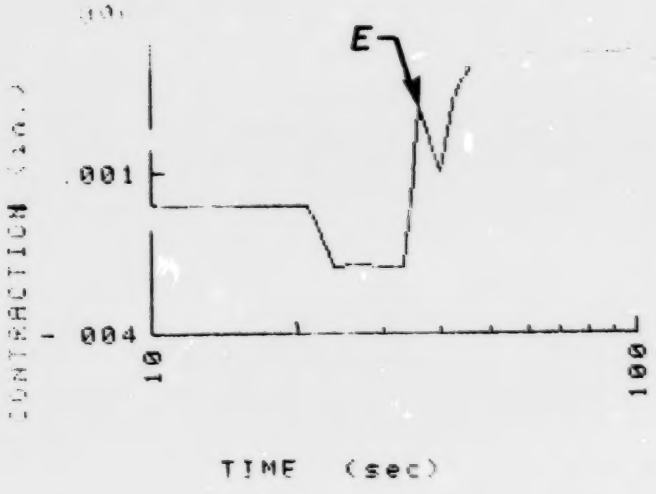

Figure 6. Contraction versus time for weld 2 as measured by LVDT 10. The arrow at E is representative of the expected behaviour when cracking occurs during the data acquisition period.

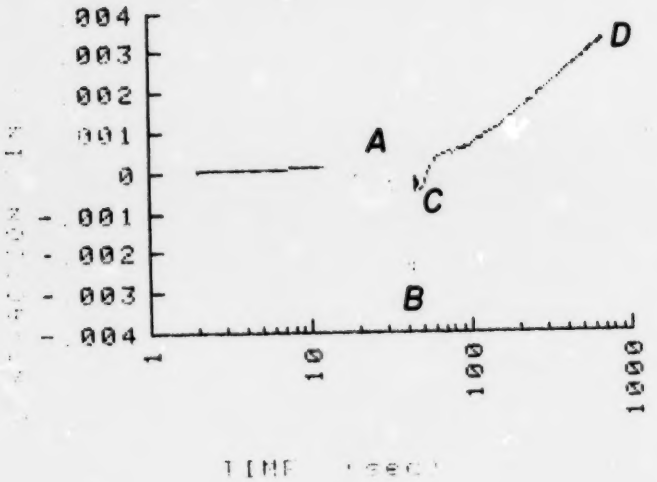

Figure 7. Contraction behaviour of a single bead which did not crack within 800 s.

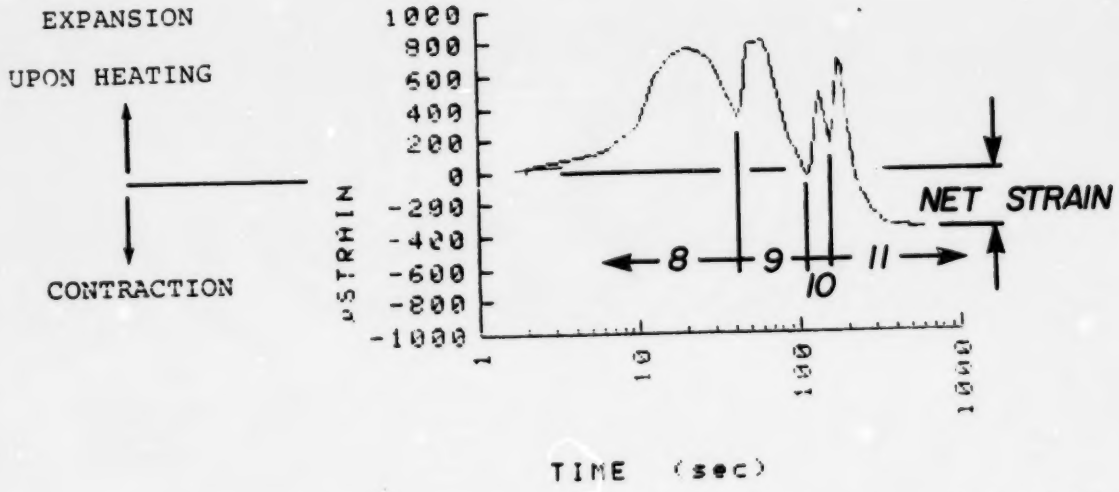

Figure 8. Strain output from strain bridge 1 during deposition of the third layer of weld 7.

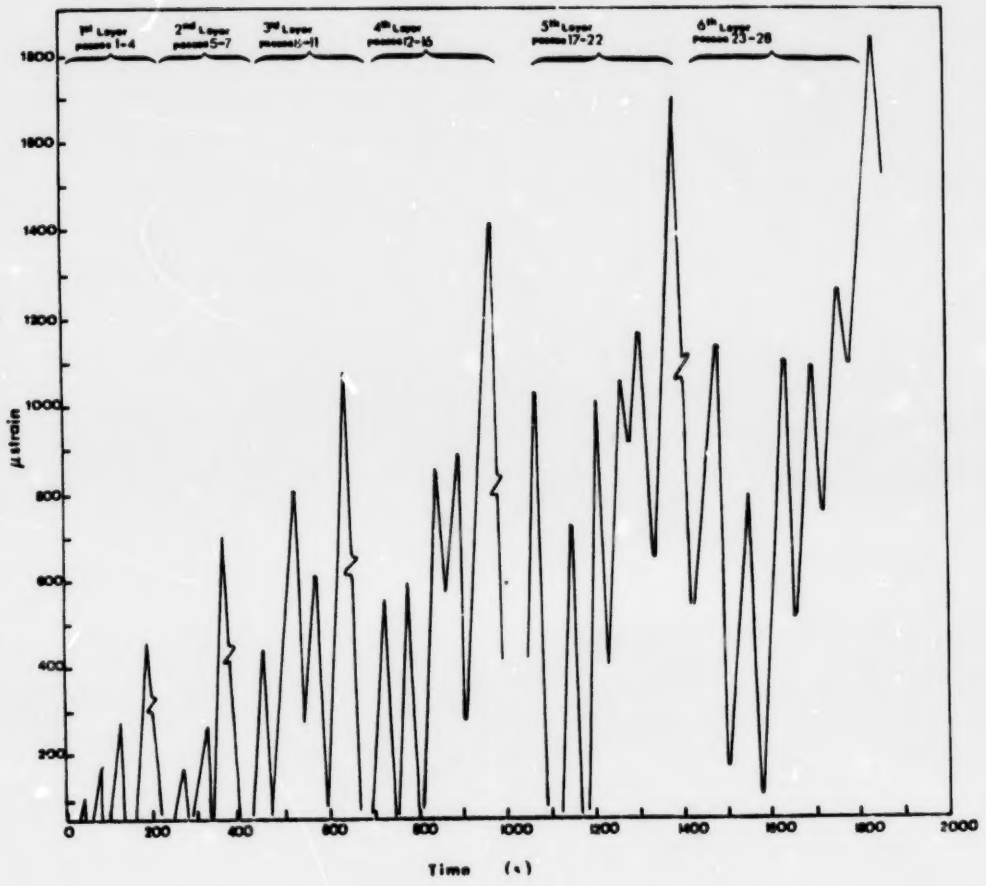

Figure 9. Net strain versus time for weld 7, multilayer SMAW deposit, as recorded by strain bridge 1.

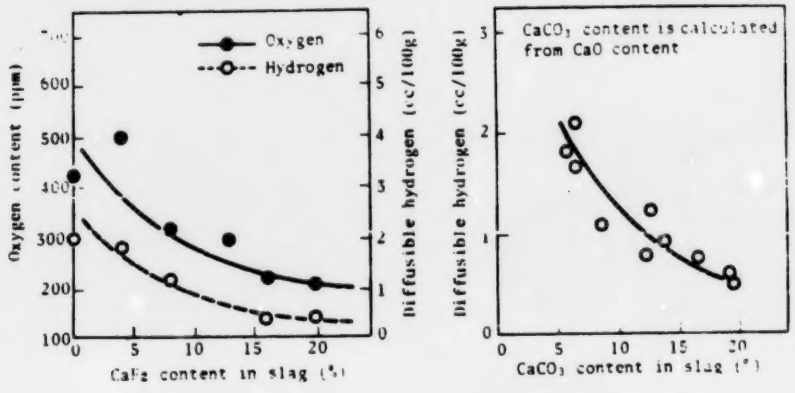

Figure 10. Relationship between CaF_2 and $CaCO_3$ content in slag and diffusible hydrogen content in weld metal (7).

APPENDIX A

Contraction versus time graphs for Welds 1 to 6.

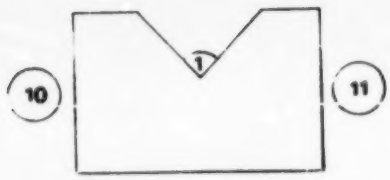

WELD I

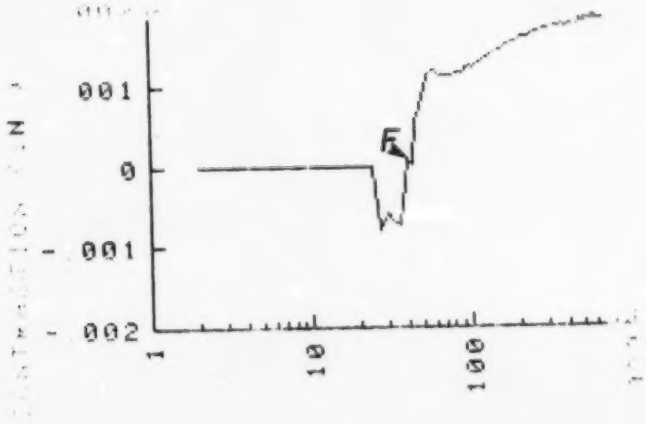

LVDT 10

TIME (sec)

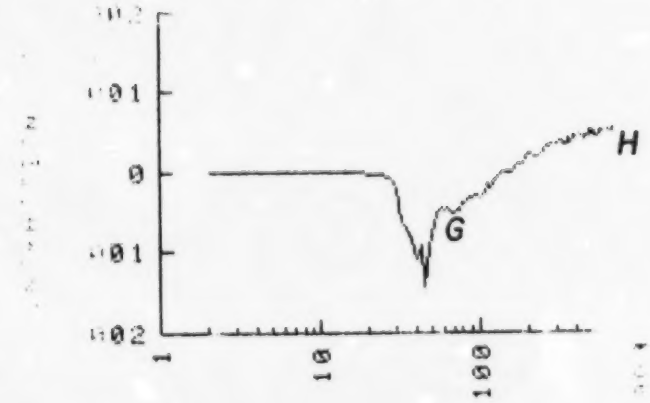

LVDT II

TIME (sec)

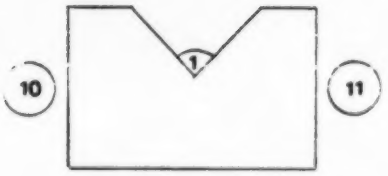

WELD 2

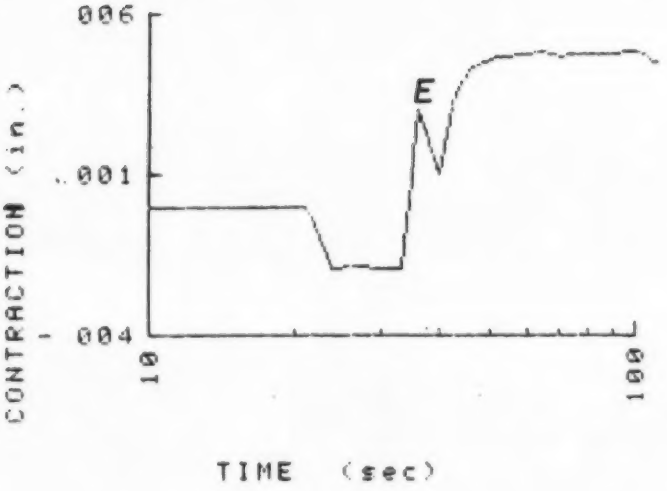

LVDT 10

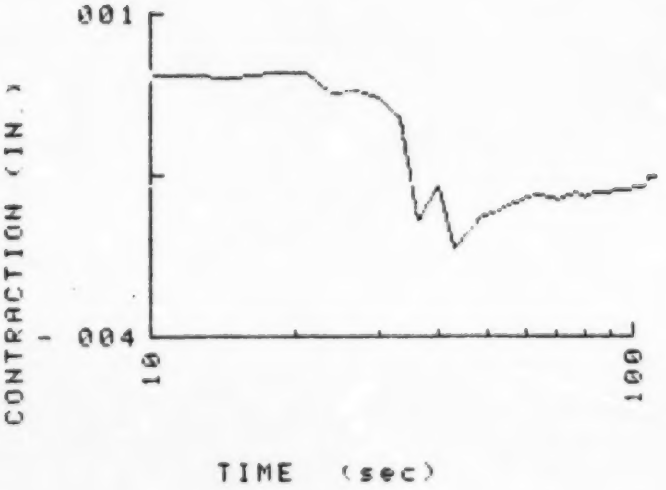

LVDT 11

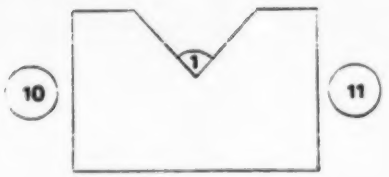

WELD 3

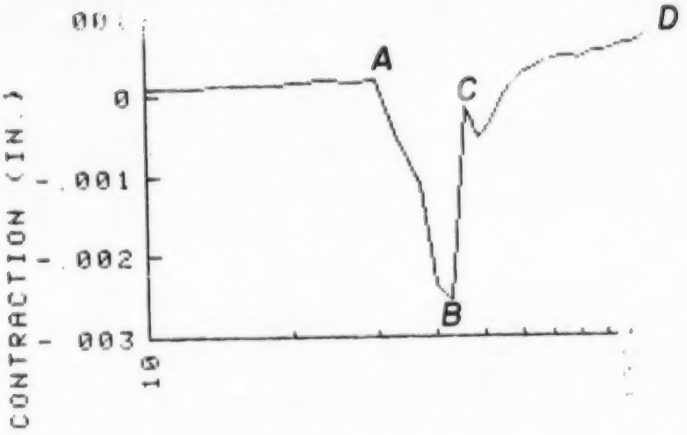

LVDT 10

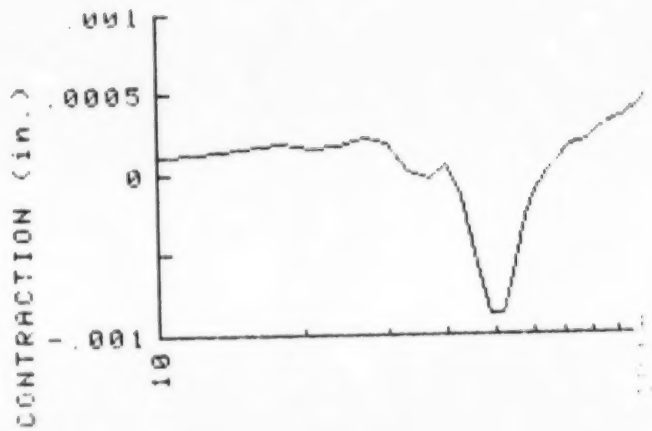

LVDT 11

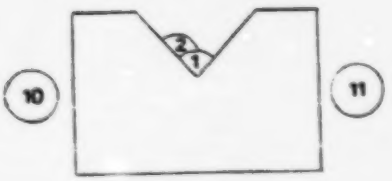

WELD 4

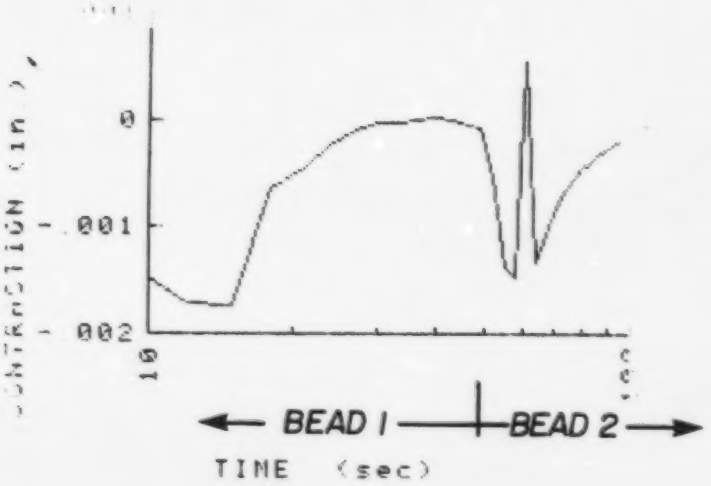

LVDT 10

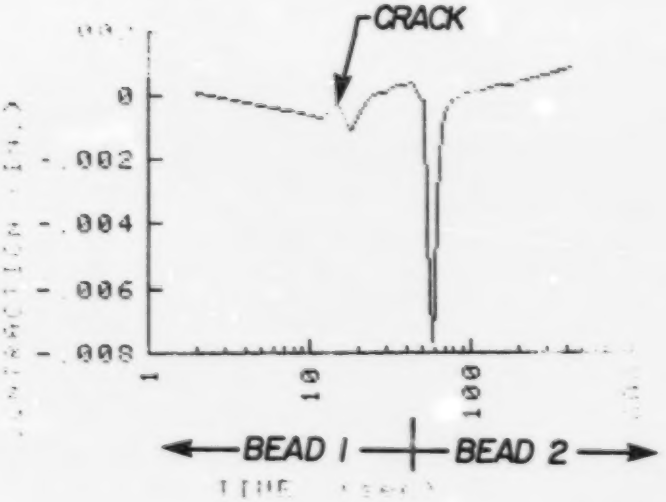

LVDT 11

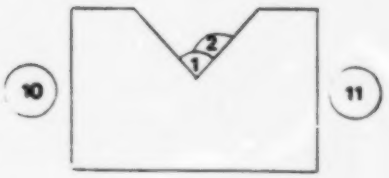

WELD 5

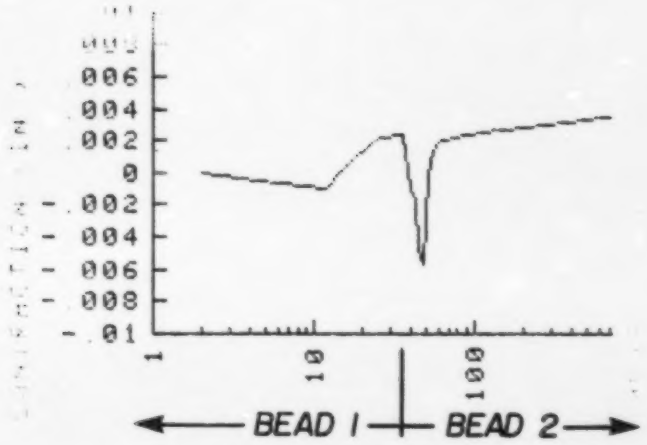

LVDT 10

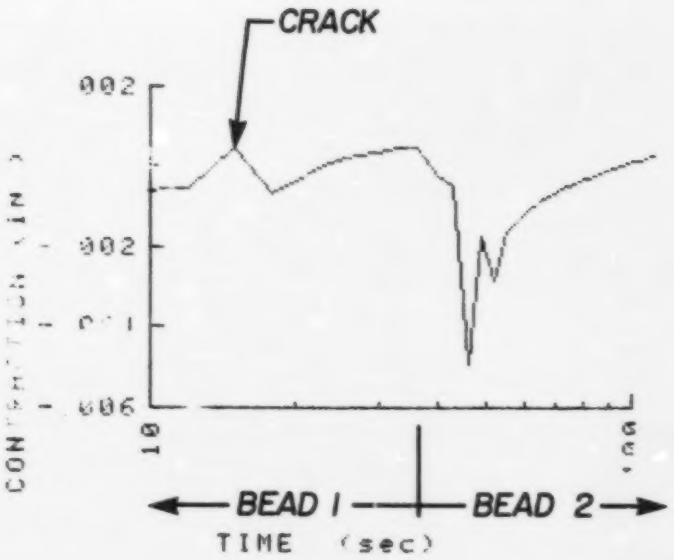

LVDT 11

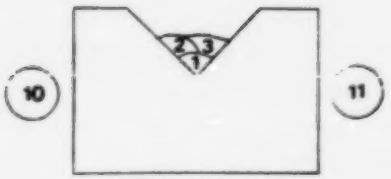

WELD 6

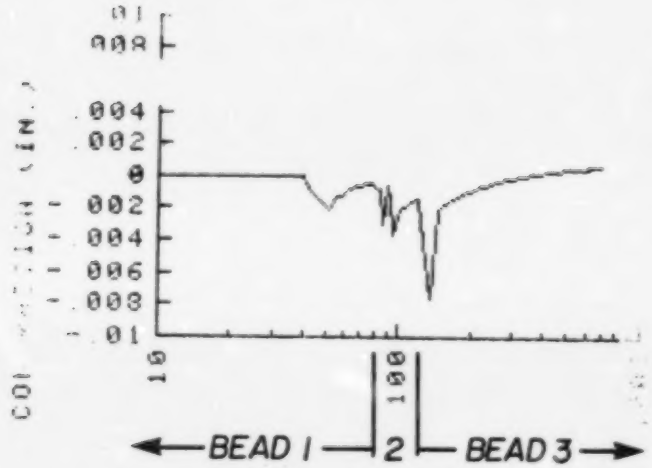

LVDT 10

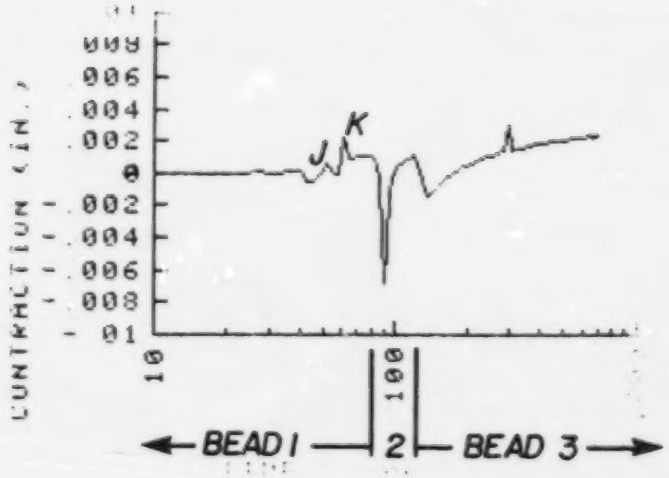

LVDT 11

APPENDIX B

Results for Weld 7.

APPENDIX B

WELDING PROCEDURE FOR WELD 7

Pass	Side	Process	Current (Amperes)	Voltage (volts)	Travel Speed (cm/min)
1	1	SMAW	140	21	18
2	1	SMAW	140	21	18
3	1	SMAW	140	21	18
4	1	SMAW	140	21	18
	1	SMAW	140	21	18
	1	SMAW	140	21	18
28	1	SMAW	140	21	18

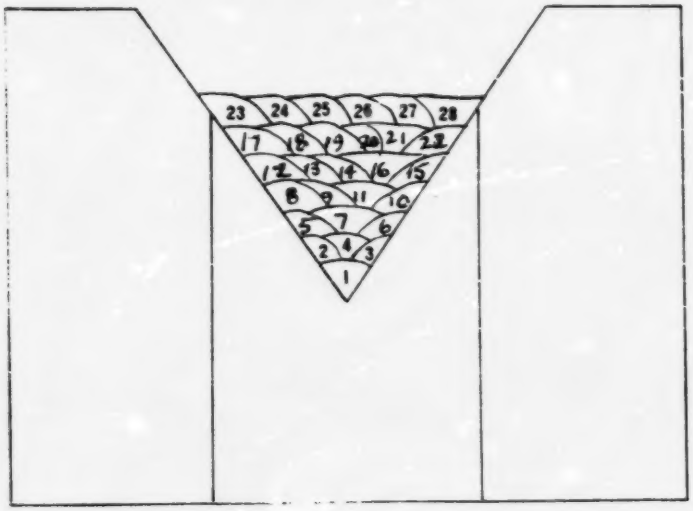

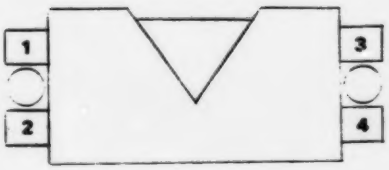

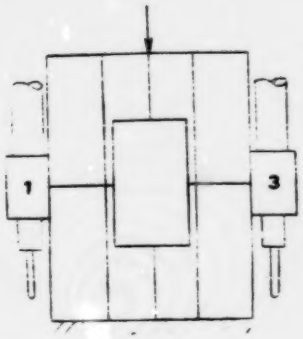

APPENDIX B

STRAIN MEASUREMENTS FOR WELD 7

File	Pass	Layer	Compressive Strain Values			
			Bridge 1	Bridge 2	Bridge 3	Bridge 4
7A	1	1	120	12	105	300
	2	1	150	33	160	420
	3	1	280	92	330	570
	4	1	430	98	400	560
7B	5	2	150	25	160	320
	6	2	350	82	260	400
	7	2	720	135	560	770
7C	8	3	440	80	230	230
	9	3	850	130	500	600
	10	3	320	70	320	270
	11	3	1050	180	850	830
7D	12	4	500	70	250	170
	13	4	800	88	380	310
	14	4	960	100	500	470
	15	4	310	65	450	170
	16	4	1120	210	1200	770
7E	17	5	700	50	230	80
	18	5	750	60	340	80
	19	5	1030	120	600	260
	20	5	700	90	510	270
	21	5	290	48	500	110
	22	5	1050	200	1500	600
7F	23	6	640	18	230	180
	24	6	650	20	120	80
	25	6	1020	0	290	0
	26	6	570	0	270	0
	27	6	480	25	390	0
	28	6	700	60	1550	270

FILE 7A

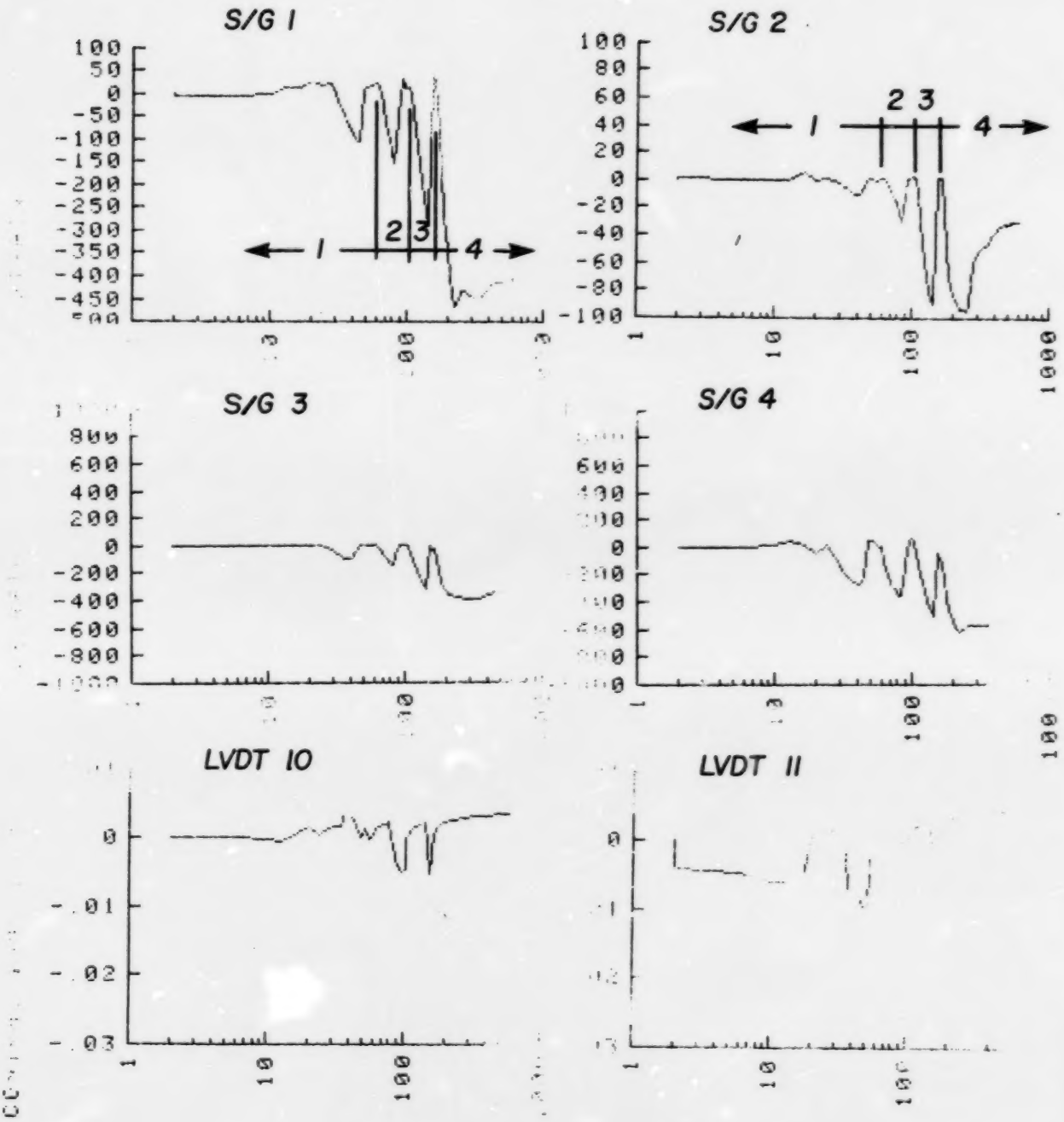
S/G 1
100
50
0
-50
-100
-150
-200
-250
-300
-350
-400
-450
1
2 3
4
S/G 2
100
80
60
40
20
0
-20
-40
-60
-80
-100
1
2 3
4
1
10
100
1000
S/G 3
800
600
400
200
0
-200
-400
-600
-800
S/G 4
600
0
100
LVDT 10
0
-.01
-.02
-.03
1
10
100
LVDT 11
0
1
10

FILE 7B

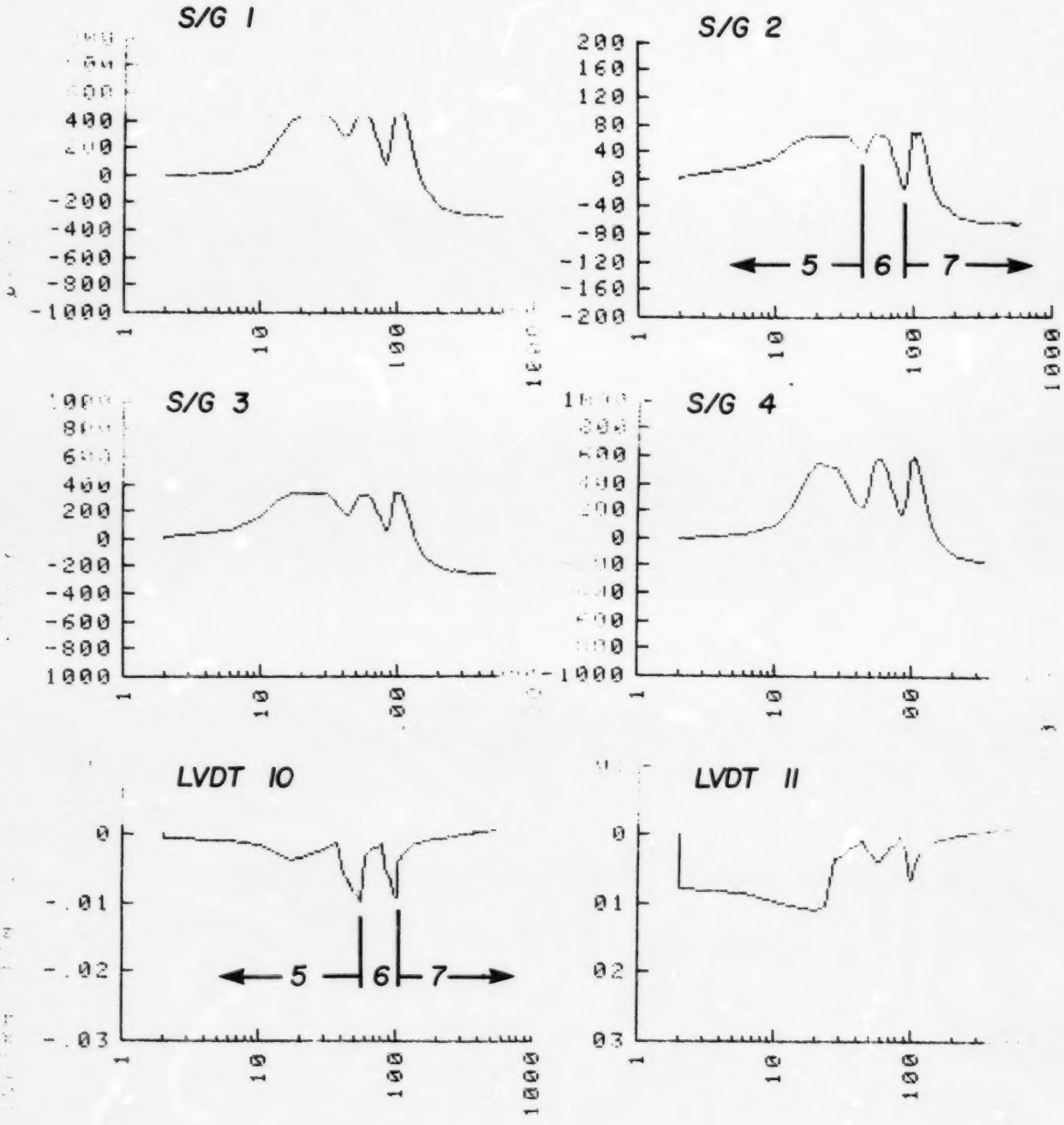

FILE 7C

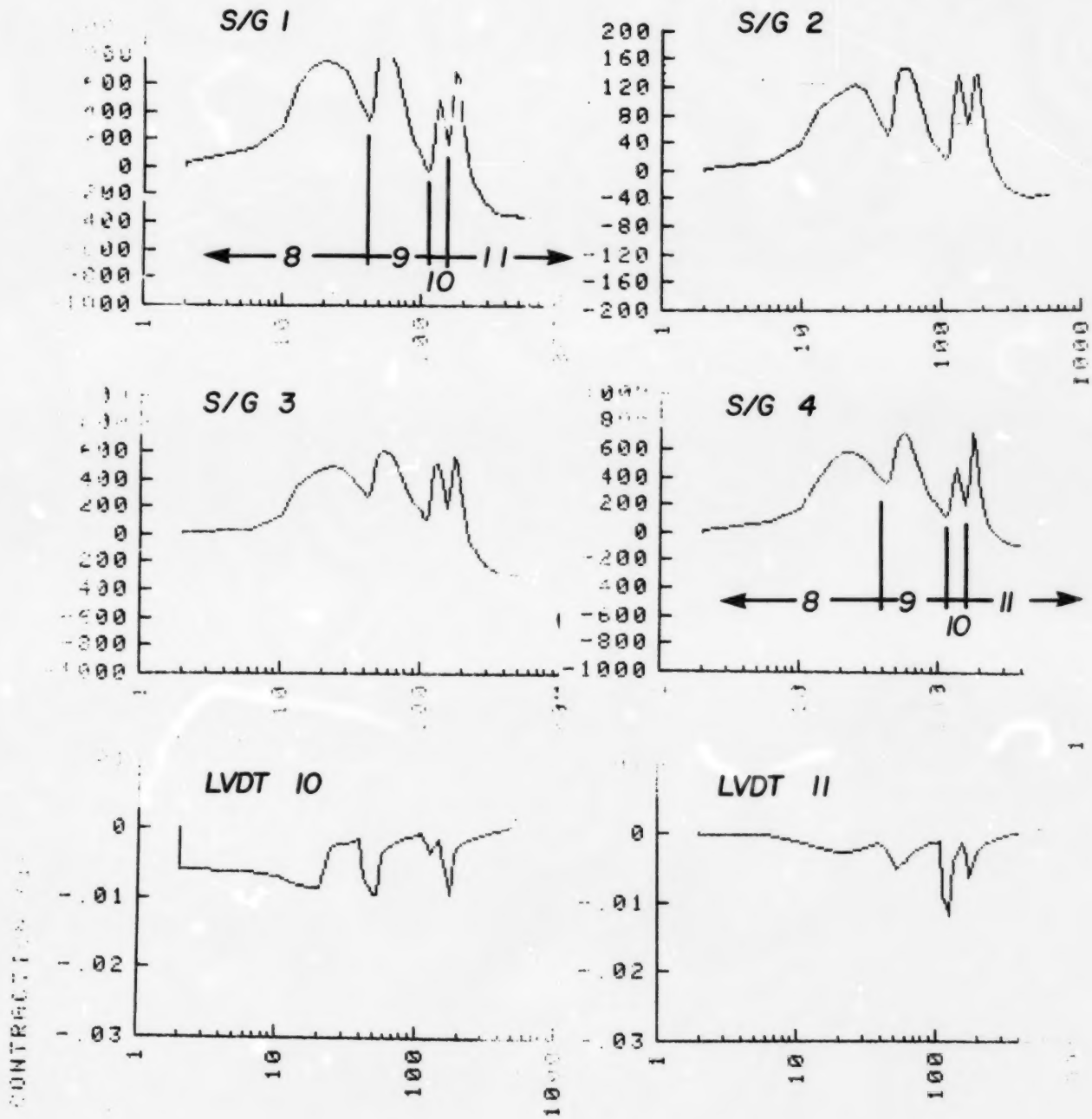
S/G 1
S/G 2
S/G 3
S/G 4
LVDT 10
LVDT 11
8
9
10
11
200
160
120
80
40
0
-40
-80
-120
-160
-200
600
400
-400
-600
-800
-1000
-.01
-.02
-.03
1
10
100
1000

FILE 7D

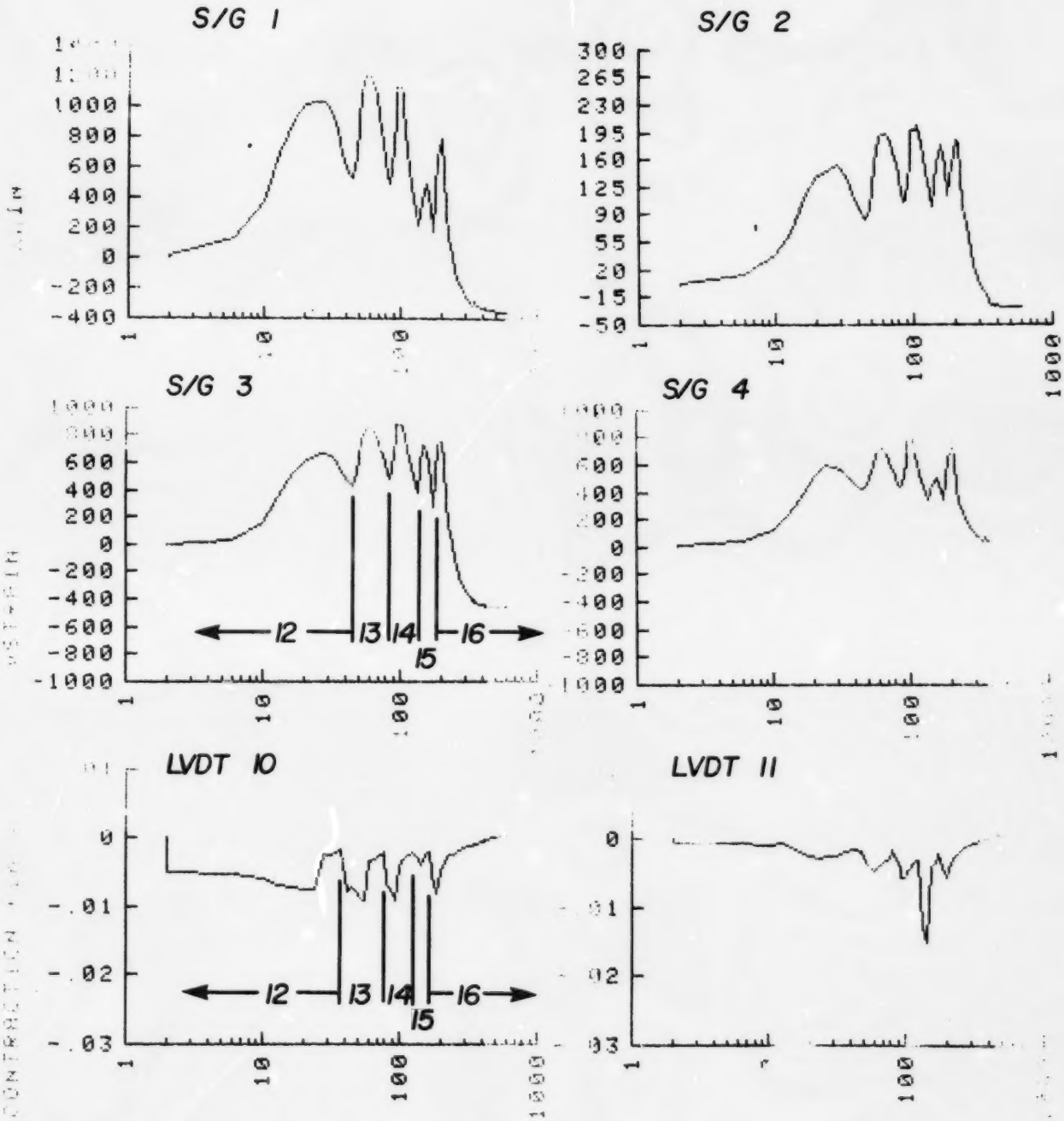

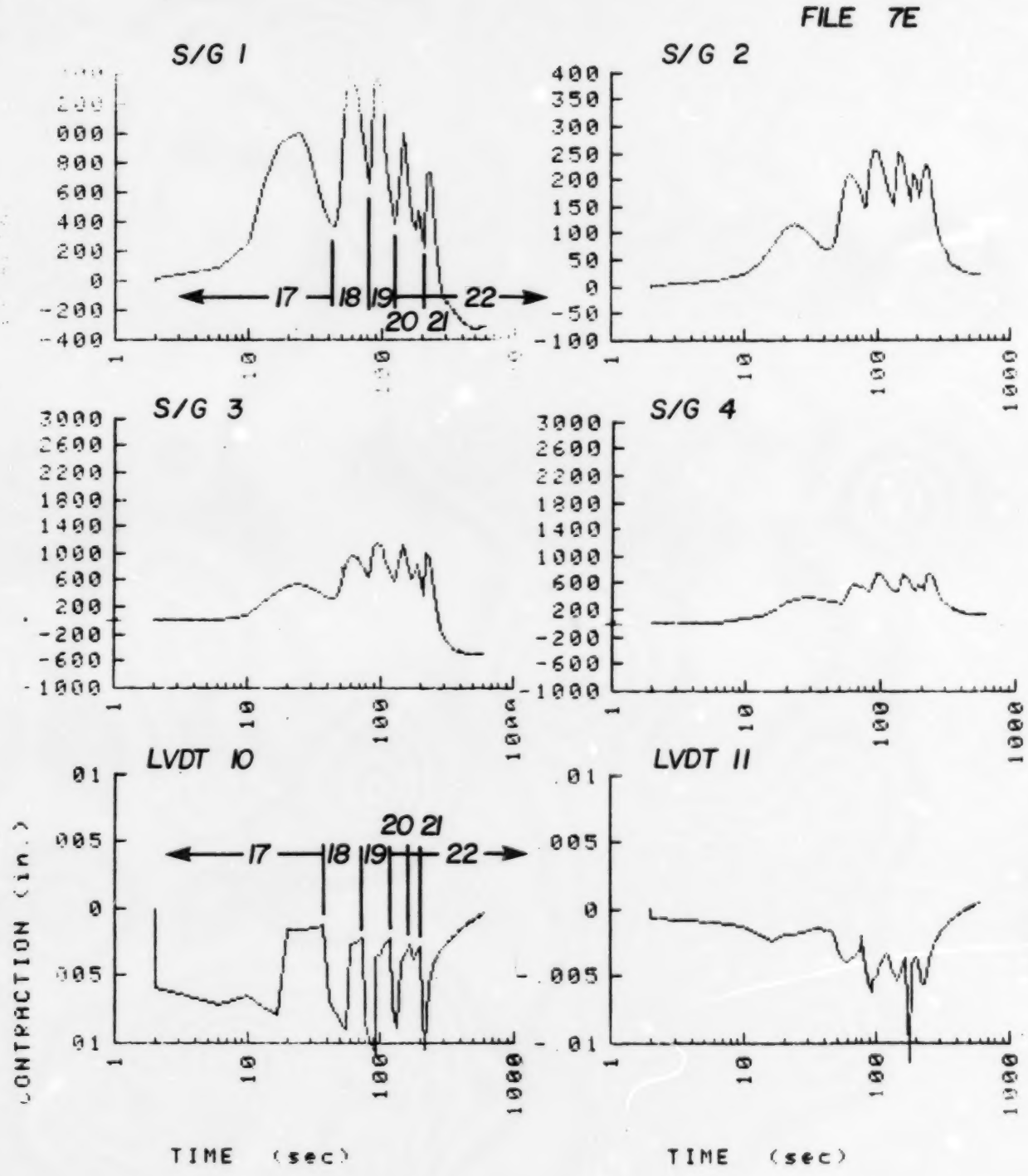
FILE 7E
S/G 1
S/G 2
S/G 3
S/G 4
LVDT 10
LVDT 11
17
18
19
20
21
22
CONTRACTION (in.)
TIME (sec)
TIME (sec)

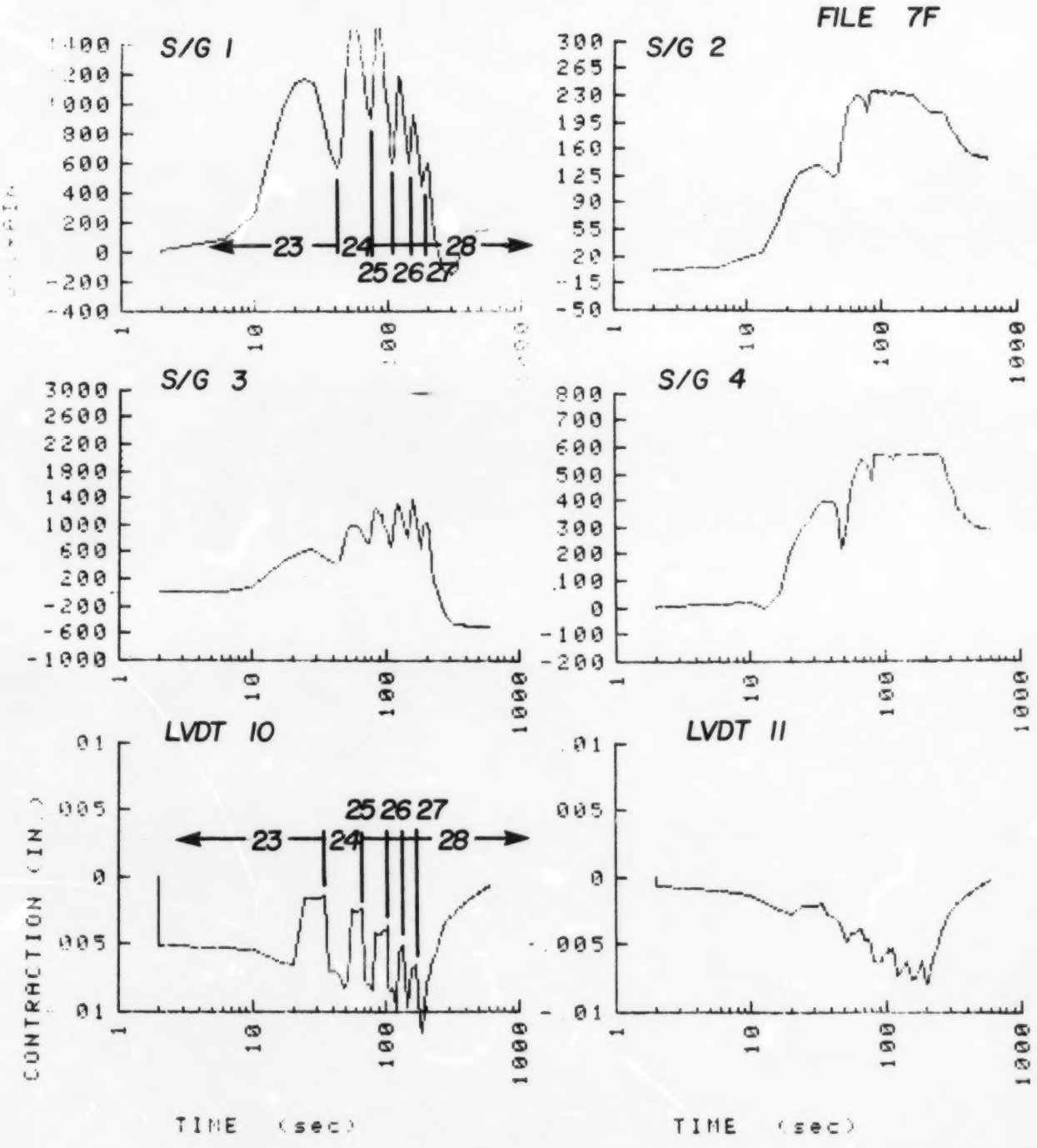
FILE 7F
S/G 1
S/G 2
S/G 3
S/G 4
LVDT 10
LVDT 11
23
24
25 26 27
28
CONTRACTION (IN.)
TIME (sec)
TIME (sec)

APPENDIX C

Welding Procedure Sheets for Welds 8 to 11.

TABLE C1
WELDING PROCEDURE FOR WELD 8

Pass	Process	Current (Amperes)	Voltage (Volts)	Travel Speed cm/min)	ESO* (mm)	Preheat/ Interpass Temp (°C)
1	SAW	450	32	40	25-30	175
2	SAW	500	32	40	"	200
3	SAW	500	32	40	"	200
↓	↓	↓	↓	↓	↓	↓
48	SAW	500	32	40	"	200

* ESO - electrical stick-out.

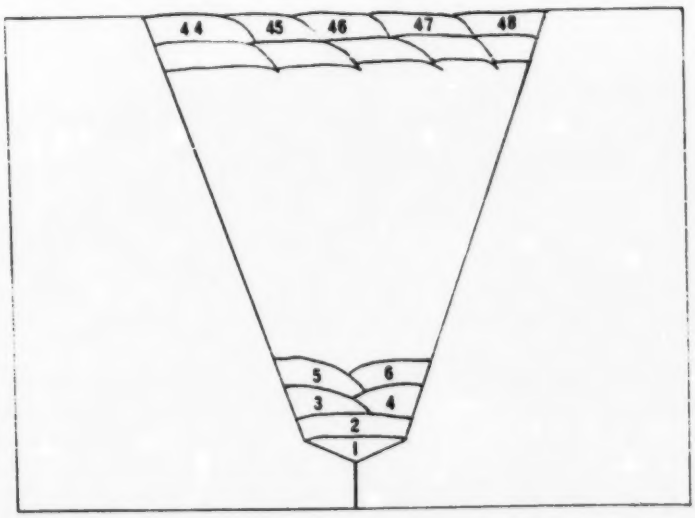

TABLE C2

WELDING PROCEDURE FOR WELD 9

Pass	Side	Process	Current (Amperes)	Voltage (Volts)	Travel Speed (cm/min)	ESO (mm)	Temp (°C)	Remarks
1	1	SMAW	140	21	14-17	--	200	Removed by back gouging
2	1	SMAW	140	21	18	--	200	Removed by back gouging
3	1	SMAW	140	21	18	--	200	
4	1	SAW	500	31	30	25-30	250	
5	1	SAW	550	31	30	"	"	
6	1	SAW	550	31	45	"	"	
7	1	SAW	550	31	45	"	"	
8	1	SAW	550	31	45	"	"	
9	1	SAW	550	31	35	"	"	Plate turned over and back gouged from side 2 after tnis pass.
10	2	SAW	550	31	35	"	"	
11	2	SAW	550	31	30	"	"	
12	2	SAW	550	31	30	"	"	
13	2	SAW	550	31	30	"	"	
14	2	SAW	550	31	40	"	"	
15	2	SAW	550	31	40	"	"	
52	2	SAW	550	31	40	"	"	After pass 66, left weld at 200°C over weekend
53	1	SAW	550	31	40	"	"	
85	1	SAW	550	31	40	"	"	

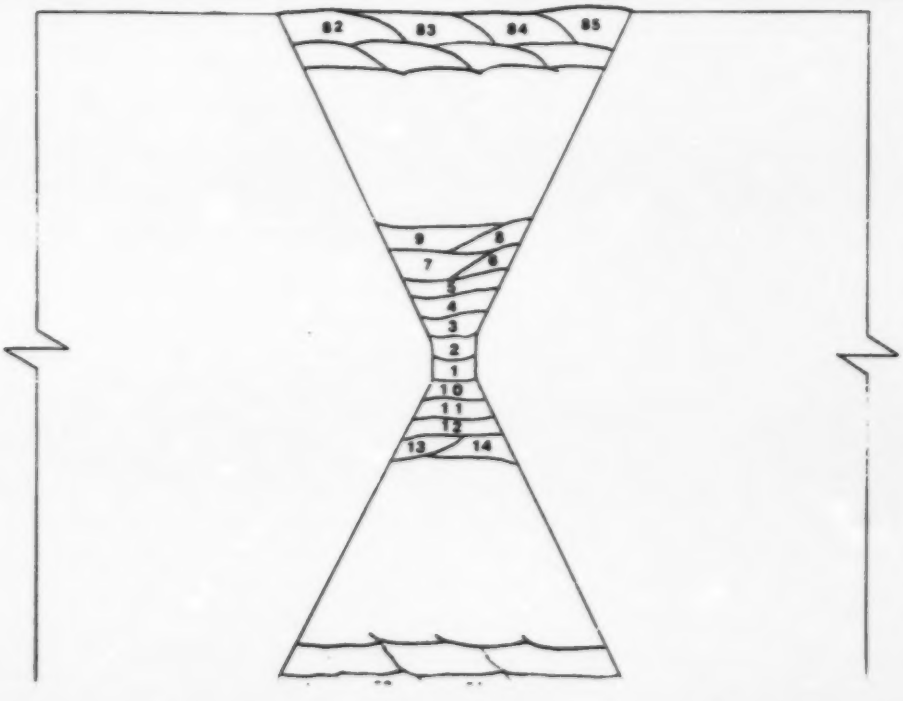

TABLE C3

WELDING PROCEDURE FOR WELD 10

Pass	Side	Process	Current (Amperes)	Voltage (Volts)	Travel Speed (cm/min)	ESO (mm)	Preheat/ Interpass Temp(°C)	Remarks
1	1	SMAW	140		14-17	-	250	
2	1	SMAW	140		18	-	250	
3	1	SMAW	140		18	-	250	
4	1	SAW	550	31	40	25-32	250	
5	1	SAW	550	31	40	"	250	
6	1	SAW	550	31	40	"	250	
7	1	SAW	550	31	40	"	250	Plate turned over and back gouged from side 2 after this pass.
8	2	SAW	550	31	40	"	100	
9	2	SAW	550	31	40	"	100	
10	2	SAW	550	31	40	"	100	
	2	SAW	550	31	40	"	100	
	2	SAW	550	31	40	"	100	
25	2	SAW	550	31	40	"	100	
26	1	SAW	550	31	40	"	100	
	1	SAW	550	31	40	"	100	After 27, left plates at 100°C over weekend.
	1	SAW	550	31	40	"	100	
57	1	SAW	550	31	40	"	100	
58	2	SAW	550	31	40	"	100	
59	2	SAW	550	31	40	"	100	
	2	SAW	550	31	40	"	100	
	2	SAW	550	31	40	"	100	
73	2	SAW	550	31	40	"	100	

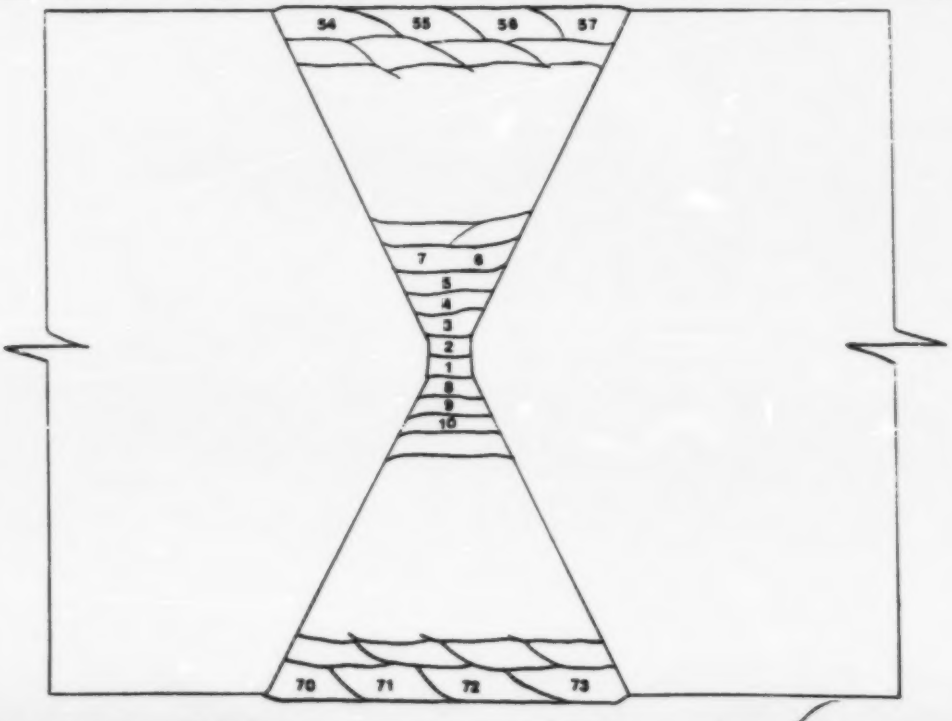

TABLE C4

WELDING PROCEDURE FOR WELD 11

Pass	Side	Process	Current (Amperes)	Voltage (Volts)	Travel Speed (cm/min)	ESO (mm)	Preheat/ Interpass Temp (°C)
1	1	SMAW	140	21	14 - 17	-	100
2	1	SMAW	140	21	18	-	100
3	1	SMAW	140	21	18	-	100
4	1	SAW	550	31	40	25-30	125
‖	1	SAW	550	31	40	"	125
‖	1	SAW	550	31	40	"	125
68	1	SAW	550	31	40	"	125